CHARGE AND CURRENT DENSITY DISTRIBUTIONS ON MODERATELY THICK TRANSMITTING CROSSED-MONOPOLE ANTENNAS

William Edward Beyatte

Report Number NPS62Zn76121

NAVAL POSTGRADUATE SCHOOL
Monterey, California

THESIS

CHARGE AND CURRENT DENSITY DISTRIBUTIONS
ON MODERATELY THICK TRANSMITTING
CROSSED-MONOPOLE ANTENNAS

by

William Edward Beyatte

December 1976

Thesis Advisor: R. W. Burton

Prepared for: Air Force Weapons Laboratory/PRP
Kirtland AFB
New Mexico 87117

UNCLASSIFIED

SECURITY CLASSIFICATION OF THIS PAGE (When Data Entered)

REPORT DOCUMENTATION PAGE		READ INSTRUCTIONS BEFORE COMPLETING FORM
1. REPORT NUMBER NPS62Zn76121	2. GOVT ACCESSION NO.	3. RECIPIENT'S CATALOG NUMBER
4. TITLE (and Subtitle) CHARGE AND CURRENT DENSITY DISTRIBUTIONS ON MODERATELY THICK TRANSMITTING CROSSED-MONOPOLE ANTENNAS		5. TYPE OF REPORT & PERIOD COVERED Final Report 1 Apr 76 - 1 Dec 76 6. PERFORMING ORG. REPORT NUMBER
7. AUTHOR(s) William E. Beyatte in conjunction with Robert W. Burton		8. CONTRACT OR GRANT NUMBER(s)
9. PERFORMING ORGANIZATION NAME AND ADDRESS Naval Postgraduate School Monterey, California		10. PROGRAM ELEMENT, PROJECT, TASK AREA & WORK UNIT NUMBERS
11. CONTROLLING OFFICE NAME AND ADDRESS Air Force Weapons Laboratory/PRP Kirtland AFB New Mexico 87117		12. REPORT DATE December 1976 13. NUMBER OF PAGES 100
14. MONITORING AGENCY NAME & ADDRESS(if different from Controlling Office)		15. SECURITY CLASS. (of this report) Unclassified 15a. DECLASSIFICATION/DOWNGRADING SCHEDULE

16. DISTRIBUTION STATEMENT (of this Report)

Approved for public release, distribution unlimited.

17. DISTRIBUTION STATEMENT (of the abstract entered in Block 20, if different from Report)

18. SUPPLEMENTARY NOTES

19. KEY WORDS (Continue on reverse side if necessary and identify by block number)

Surface Charge and Current Distribution
Crossed-Monopole
Junction Charge

20. ABSTRACT (Continue on reverse side if necessary and identify by block number)

Charge and current density distributions in the vicinity of the cross junction of several configurations of electrically long, moderately thick, crossed-monopole antennas with an intersecting angle of 45 degrees were measured. The recorded data was compared with a monopole antenna with the same dimensions as the vertical segment

DD FORM 1 JAN 73 1473 EDITION OF 1 NOV 65 IS OBSOLETE
S/N 0102-014-6601 |
(Page 1)

UNCLASSIFIED

SECURITY CLASSIFICATION OF THIS PAGE (When Data Entered)

of the crossed monopole. Junction conditions such that there would be a maximum current/minimum charge and minimum current/maximum charge on the vertical monopole were investigated.

Charge and Current Density Distributions on Moderately Thick Transmitting Crossed-Monopole Antennas

by

William Edward Beyatte
Lieutenant, United States Navy
B.E.E.E. Vanderbilt University, 1970

Submitted in partial fulfillment of the
requirements for the degree of

MASTER OF SCIENCE IN ELECTRICAL ENGINEERING

from the
NAVAL POSTGRADUATE SCHOOL
December 1976

NAVAL POSTGRADUATE SCHOOL
Monterey, California

Rear Admiral Isham W. Linder
Superintendent

Jack R. Borsting
Provost

This thesis was prepared in conjunction with research supported in part by AFWL/PRP under Project numbers 75-002 and 76-211. Reproduction of all or part of this report is authorized.

Released as a
technical report by:

ABSTRACT

Charge and current density distributions in the vicinity of the cross junction of several configurations of electrically long, moderately thick, crossed-monopole antennas with an intersecting angle of 45 degrees were measured. The recorded data was compared with a monopole antenna with the same dimensions as the vertical segment of the crossed-monopole. Junction conditions such that there would be a maximum current/minimum charge and minimum current/maximum charge on the vertical monopole were investigated.

TABLE OF CONTENTS

ACKNOWLEDGEMENT

The author is sincerely grateful to Associate Professor Robert W. Burton for his professional guidance, dedicated counsel and continual support during the preparation of this thesis. Other members of the Naval Postgraduate School staff who provided valuable assistance include Mr. Frank Abbe, Mr. Robert Moeller, and ET1 Thomas Nowak. Finally, the completion of this thesis is due in no small part to the moral support provided by the author's wife, Gail.

I. INTRODUCTION

A. BACKGROUND

The charge and current density distributions on the conducting surfaces of complex structures are the basis for understanding how those structures would function as antennas. Two structures which have been investigated in recent years are the crossed-monopole and crossed-dipole antennas (Figure 1). The motivation for studying these two antenna configurations has been their use as models in determining the effects on fixed wing aircraft of exposure to the Electromagnetic Pulse (EMP) associated with detonation of a nuclear weapon. Electric field intensities as high as 100,000 volts/meter from a high level nuclear explosion pose a threat to the electronic and electrical systems aboard aircraft, missiles, and surface installations [DNA Report No. 2772T]. The broad spectrum electromagnetic pulse can excite large standing waves on structures at specific frequencies determined by the physical dimensions of the object. Aircraft at high altitudes, thousands of miles from the nuclear burst, would be vulnerable to EMP effects from a high altitude burst since the thin atmosphere

would absorb only a small portion of the electromagnetic energy. The possibility of large currents and charge concentrations being induced on the wings and fuselage of an aircraft has generated concern that mission effectiveness may be impaired or destroyed by the detrimental effects on internal components resulting from EMP exposure.

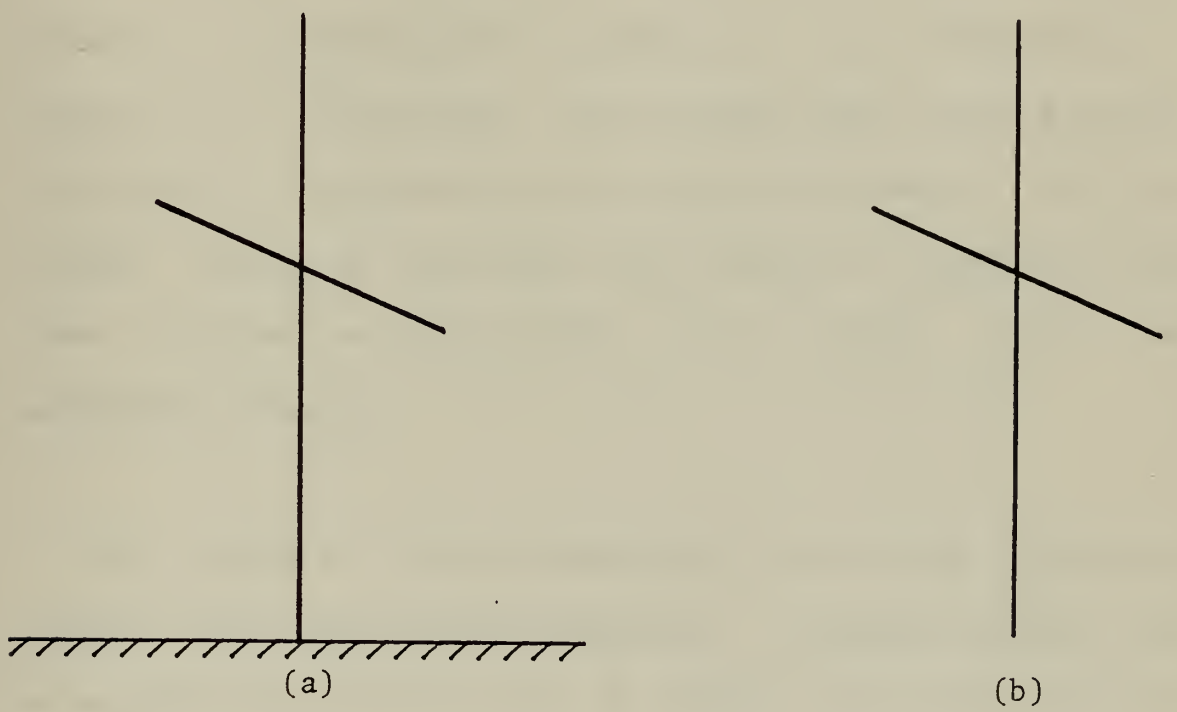

Figure 1. - (a) Crossed-monopole antenna over ground plane and (b) crossed-dipole antenna

An electrically thin crossed-dipole scattering antenna has been studied as a first approximation model to a fixed wing aircraft [Burton 1974, Burton and King 1975]. A moderately thick crossed-monopole over a ground plane has also been

used to model an aircraft [McDowell 1976]. The crossed-monopole over a ground plane does not share the same similarity with an aircraft as does the crossed-dipole, but it does allow practical experimental determination of charge and current density distributions on the conducting surface.

In addition to studying an aircraft as an unintentional gatherer of electromagnetic energy it is interesting to consider the possibility of utilizing the entire aircraft structure as a transmitting or receiving antenna. Such an antenna would be inherently low profile and would lack the usual problem of integrating the antenna into the aerodynamic design.

The study of crossed-monopoles also has importance outside the aeronautical community. A monopole antenna may be modified by addition of a cross arm with resulting changes in the monopole's radiation pattern and feed point impedance. A crossed-monopole may thus be better suited for some applications than the standard monopole. Empirical data on crossed-monoploes can also be valuable in assessing the validity of analytic solutions for charge and current distributions such as digital computer simulation programs.

B. THESIS OBJECTIVE

The object of this work was to expand the present reservior of information on crossed-monopole antennas. Charge and current density distributions on a moderately thick base driven crossed-monopole transmitting antenna with a non-orthogonal geometry were to be experimentally determined. The interaction between the two cross elements was to be analyzed using Kirchoff's Current Law, Lenz's Law, and a recent development in the understanding of junction boundary conditions [Burton and King 1975]. Also the far field radiation patterns for both orthogonal and non-orthogonal configurations were to be determined.

II. THEORY

A. MONOPOLES

Theoretical solutions for the charge and current density distributions on cylindrical monopole antennas are well established and have been proven valid in experimental work [King 1956]. The ideal monopole is assumed to have current and charge densities sinusoidually distributed along its length with an end point boundary condition of zero current and maximum charge. Figure 2 depicts assumed distributions for monopoles of various lengths. This sinusoidal (or zeroth-order) solution is a valid approximation for physically realizable antennas within certain limits. If the antenna radius is small compared to antenna height and also small when compared to the wavelength of the frequency at which it is driven then the zeroth-order solution is a close approximation to the actual distributions. Higher order solutions have been developed for a more precise assessment of the distributions on antennas when such an accurate analysis is necessary. The zeroth-order solution is adequate for analyzing the various resonant conditions and inclusion of terms necessary to account for the non-zero

minimums and other non-sinusoidual phenomena only adds unnecessary complexity to the analysis.

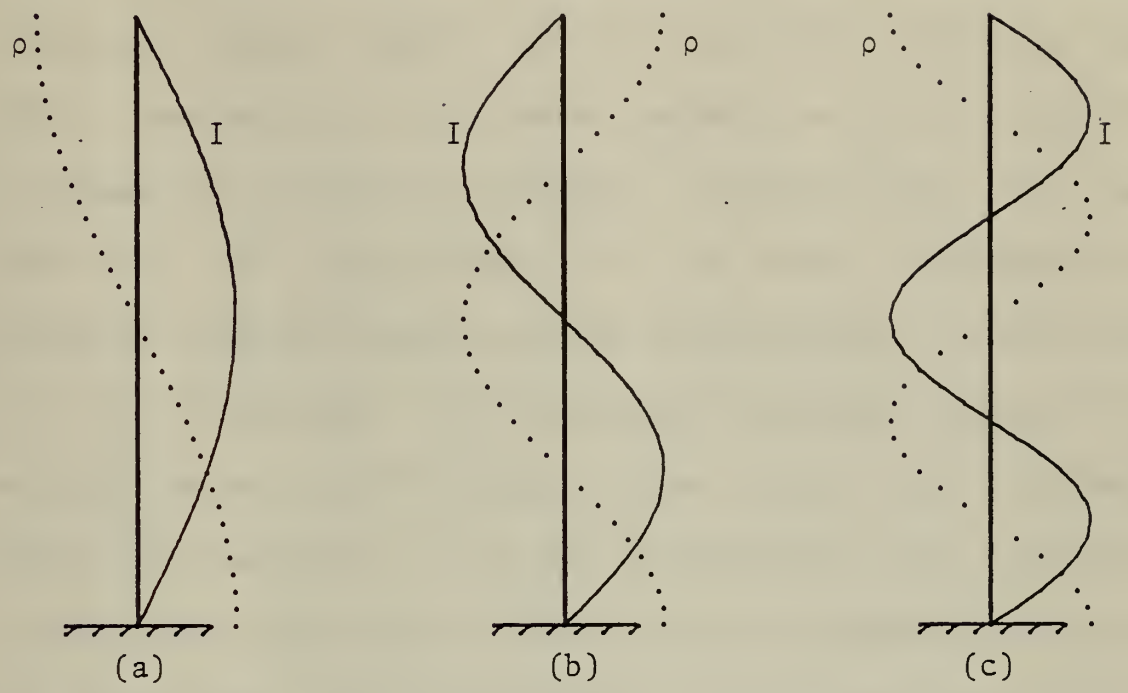

Figure 2. - Assumed charge and current density on monopoles (a) 1/2, (b) 1, (c) 3/2 wavelength in height

B. CROSSED-MONOPOLES

When two monopoles are crossed (Figure 1a) the sinusoidal distributions of charge and current no longer conform to the zeroth-order solution, particularly near the junction. Charge and current distributions on the crossed-monopole may be analyzed by considering the two major factors affecting those distributions. First, each

segment has a distribution influenced by the end point boundary conditions and tendency to establish sinusoidally varying distributions representing the zeroth-order solution. Second, forces due to inductive coupling and charge accumulation on adjacent segments serve to reinforce or oppose the natural sinusoidal distributions. If the cross arm is perpendicular to the base fed segment no inductive coupling occurs and the distributions on the cross arm are determined by the charge distributions along the vertical member and the length of the cross arm [McDowell 1976]. If the cross arm is not perpendicular then inductive coupling will also have an effect on the distributions along the cross arms. Earlier studies in this area [Burton 1974, McDowell 1976] have concentrated on crossed-monopoles with perpendicular geometry. Consideration of non-perpendicular intersections of crossed-monopole segments provides a better understanding of the general crossed-monopole configuration.

In the perpendicular case the charge standing wave pattern on the vertical element produces E field forces oriented perpendicular to the driven crossed segments; these E field variations induce currents and charge concentrations along the crossed segments. In the oblique case the forces due to charge concentrations are combined with additional

forces due to inductive coupling. The distributions on the cross arms result from the combined effect of inductive and charge related forces and are complicated by the lack of symmetry. The inductive coupling effect becomes more significant as the antenna configuration departs further from the perpendicular case. The contribution due to inductive coupling to the cross arms is more involved than the contribution due to charge concentrations since the induced currents are a function of the time rate of change of current in the driven segment, not simply current magnitudes.

III. CHARGE AND CURRENT DISTRIBUTIONS

A. EXPERIMENTAL APPARATUS

1. Antennas

Brass tubing 6.35 cm (2.5 inches) in diameter was used to construct the antennas. The diameter was sufficiently large to classify the antennas as moderately thick (the circumference was .2 wavelength at 300 Mhz, .13 wavelength at 195 Mhz) and the opening inside the tubing was large enough to accomodate the apparatus used to position the charge and current measuring devices.

a. Monopole

The reference monopole (Figure 3) was 101.5 cm in height with a .32 cm (1/8 inch) slot cut longitudinally from 30 cm above the base to 1.5 cm from the top. Correct operation of the test apparatus was verified by taking data on this antenna and comparing it with established theoretical and experimental results for monopoles [King 1956].

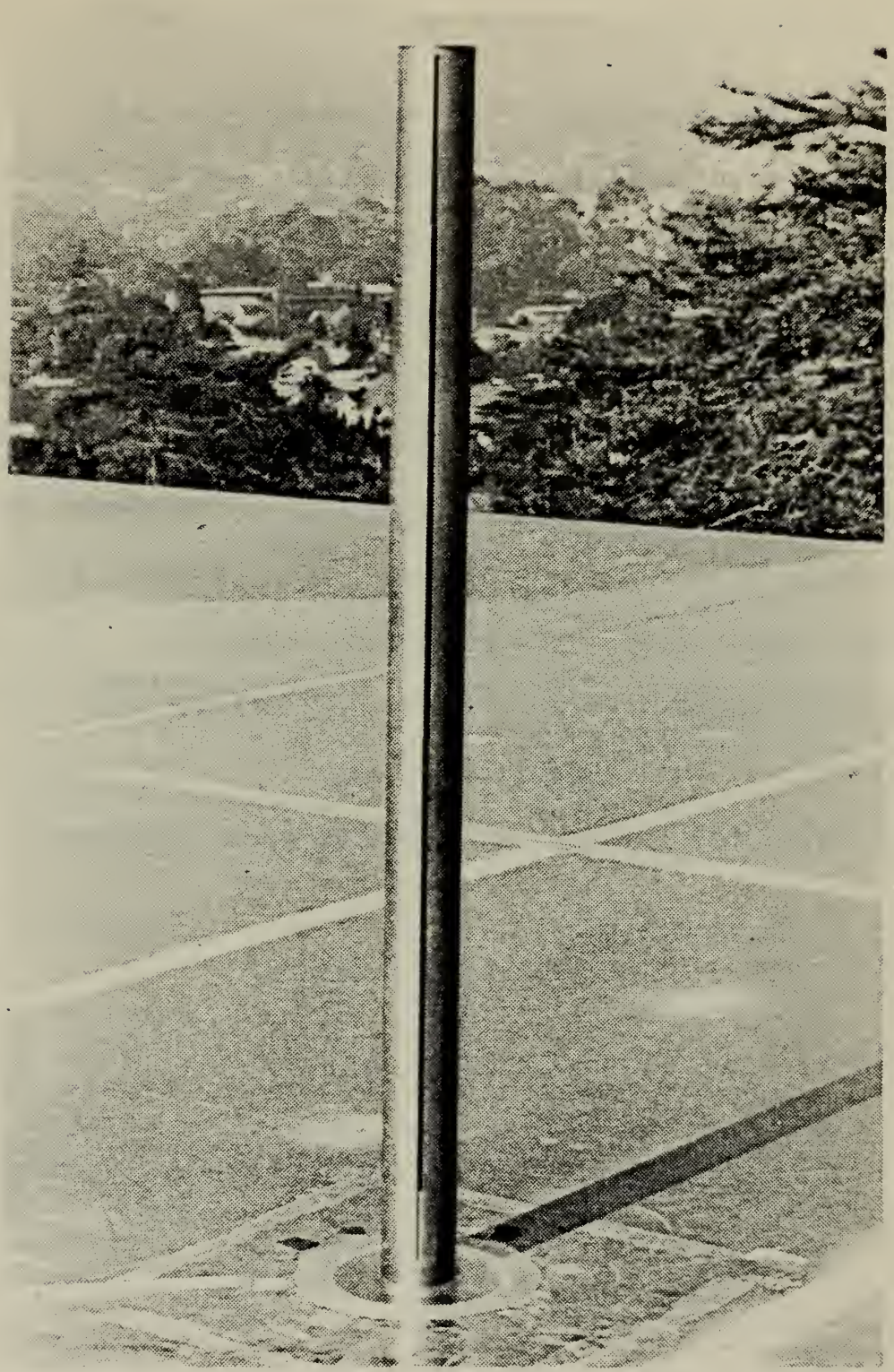

Figure 3. - Reference monopole

b. Crossed-Monopoles

The cross structure was constructed by joining two sections of brass tubing at a 45° angle (Figure 4). The vertical member extended to a height of 99 cm and the cross member measured 60 cm end to end. A .32 cm slot extended longitudinally for 30 cm from the junction center out along each segment. Additional slots were cut along the bottom of the cross segments and down the sides of the lower vertical section. A pulley was located inside the antenna at the junction to facilitate measurements along the cross segments. The pulley was suspended from a solid brass rod which extended down from a point near the top of the vertical section where a brass disc was secured inside the tubing.

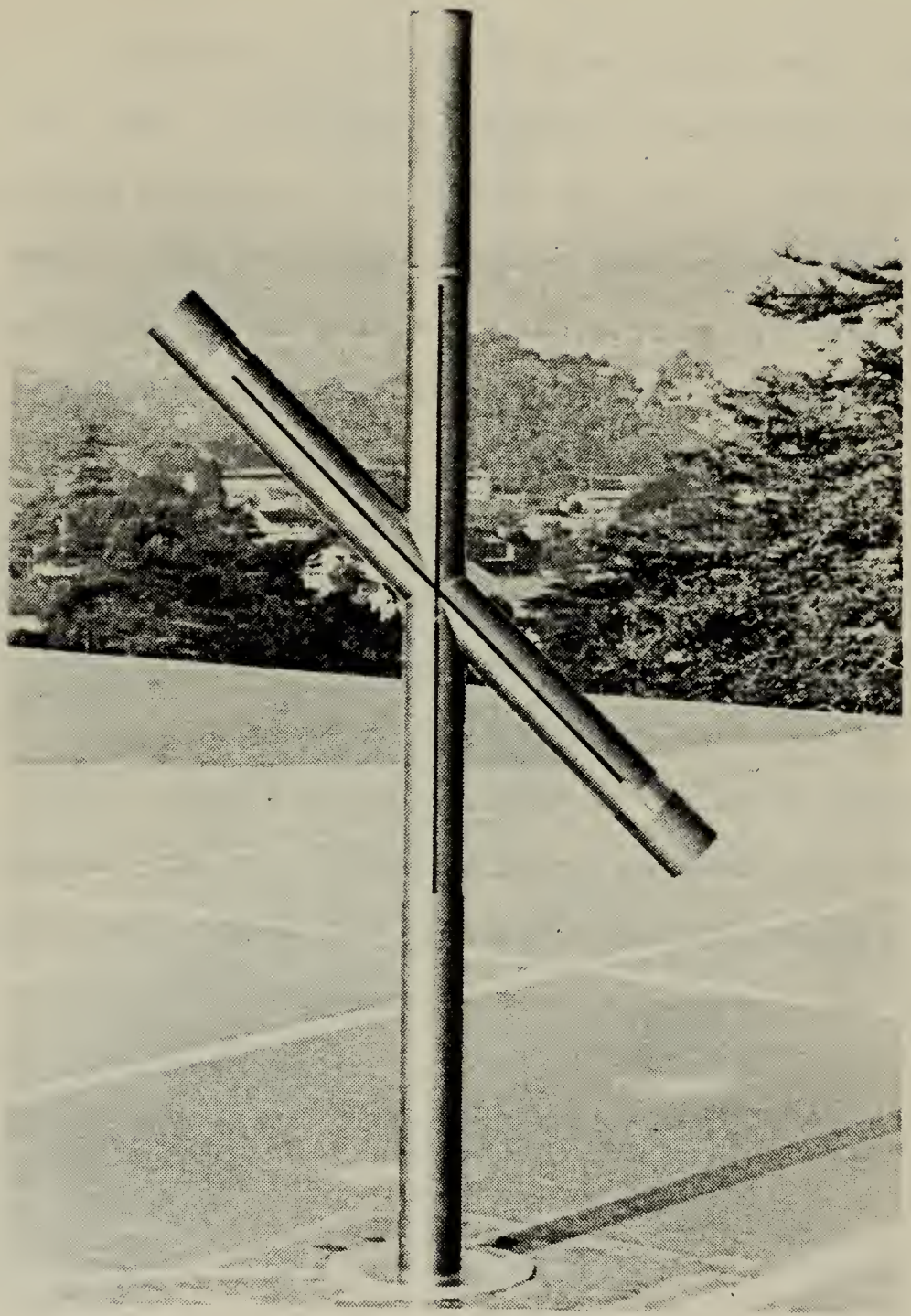

Figure 4. - Typical crossed-monopole configuration

c. Length Adjustment

Additional sections of brass tubing were fitted onto the ends of the basic antennas to vary their length. The sections were cut to lengths of 25, 7.5, 5, and 3.25 cm. Each had a slotted ring extending from one end which was machined to the inner diameter of the antenna tubing, thus the sections could be mated without introducing any significant discontinuities on the outer surface. To provide electrical continuity and additional support the junctions were covered with conductive copper or aluminum tape. Accurate length adjustment was accomplished by using standard length sections to provide approximate lengths and then custom cutting small sections of tubing to make fine adjustments. End caps were constructed to close the tubing at the antenna extremities. Figure 5 shows (clockwise from upper left) a 25 cm extension, 7.5 cm extension, end cap, and fine adjustment rings.

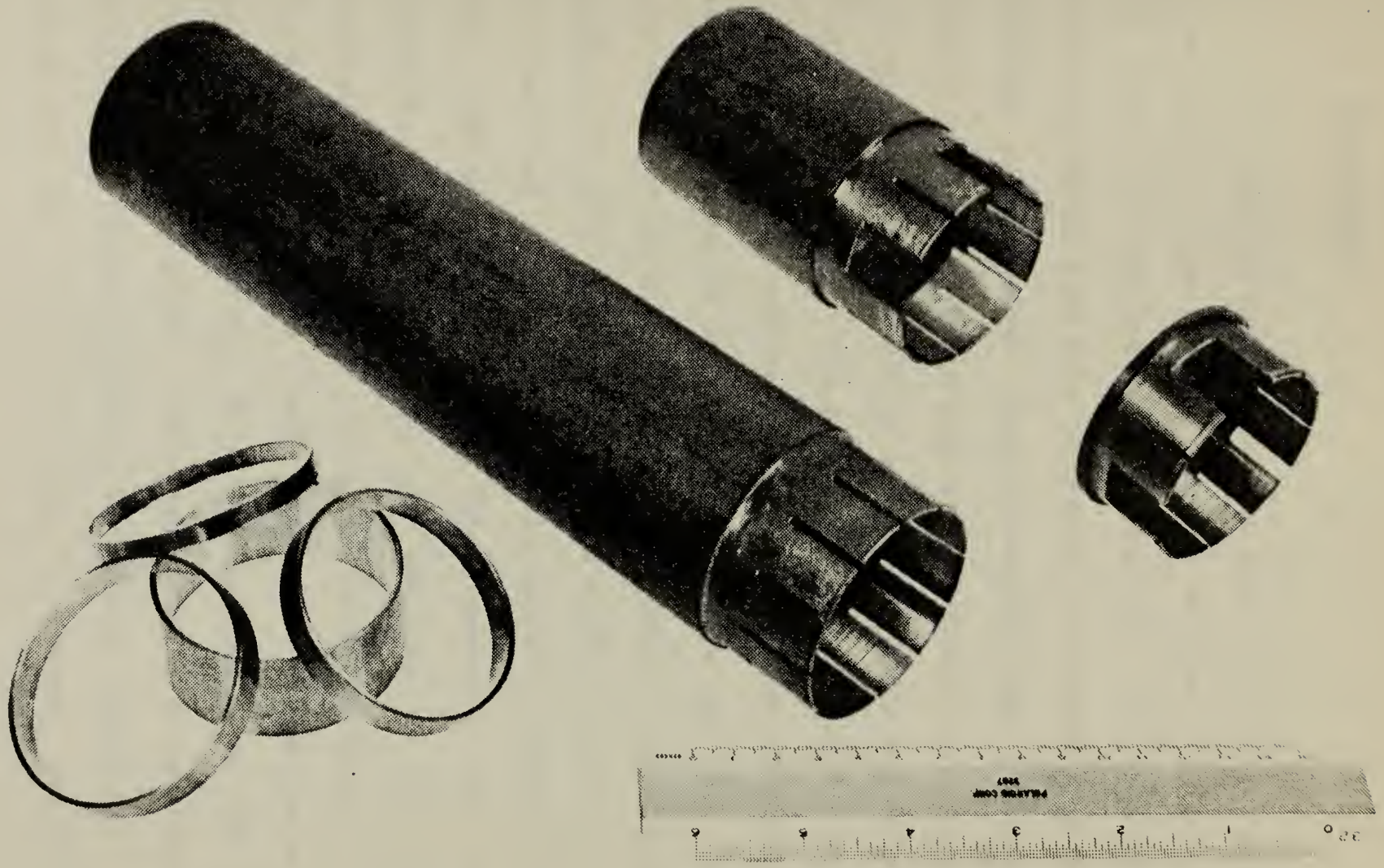

Figure 5. - Antenna extensions and end cap

2. Feed System

A feed system was required which would allow access to the inside of the crossed-monopole structure to position the charge and current measuring devices. The undesirable alternative would have been to position a probe supporting mechanism and observer above the ground plane in the near field of the antenna. The feed system (Figure 6) consisted of a short section of coaxial transmission line suitable for driving the antennas. The dimensions were chosen to provide a characteristic impedance of as near 50 ohms as possible. Two standard sizes of brass tubing (6 inch and 2.5 inch) were selected which resulted in a calculated characteristic impedance of 50.9 ohms. The aluminum flange at the top of the feed was added to match the circular opening in the image plane (discussed below). The extension of the inner conductor above the flange was machined to the inner diameter of the antenna tubing allowing antennas to be mounted. The antenna then formed a continuation of the coaxial inner conductor. RF energy was applied to the feed system via two N-type connectors located 24 cm above the base plate on opposite sides of the outer conductor. The system was fed from two sides to provide symmetrical

exitation which reduced the possibility of multiple modes of propagation within the coax. The center conductors of the N-type jacks were extended to the inner conductor of the feed system with a .32 cm brass rod. A plexiglass disc at the top to the feed supported the center conductor.

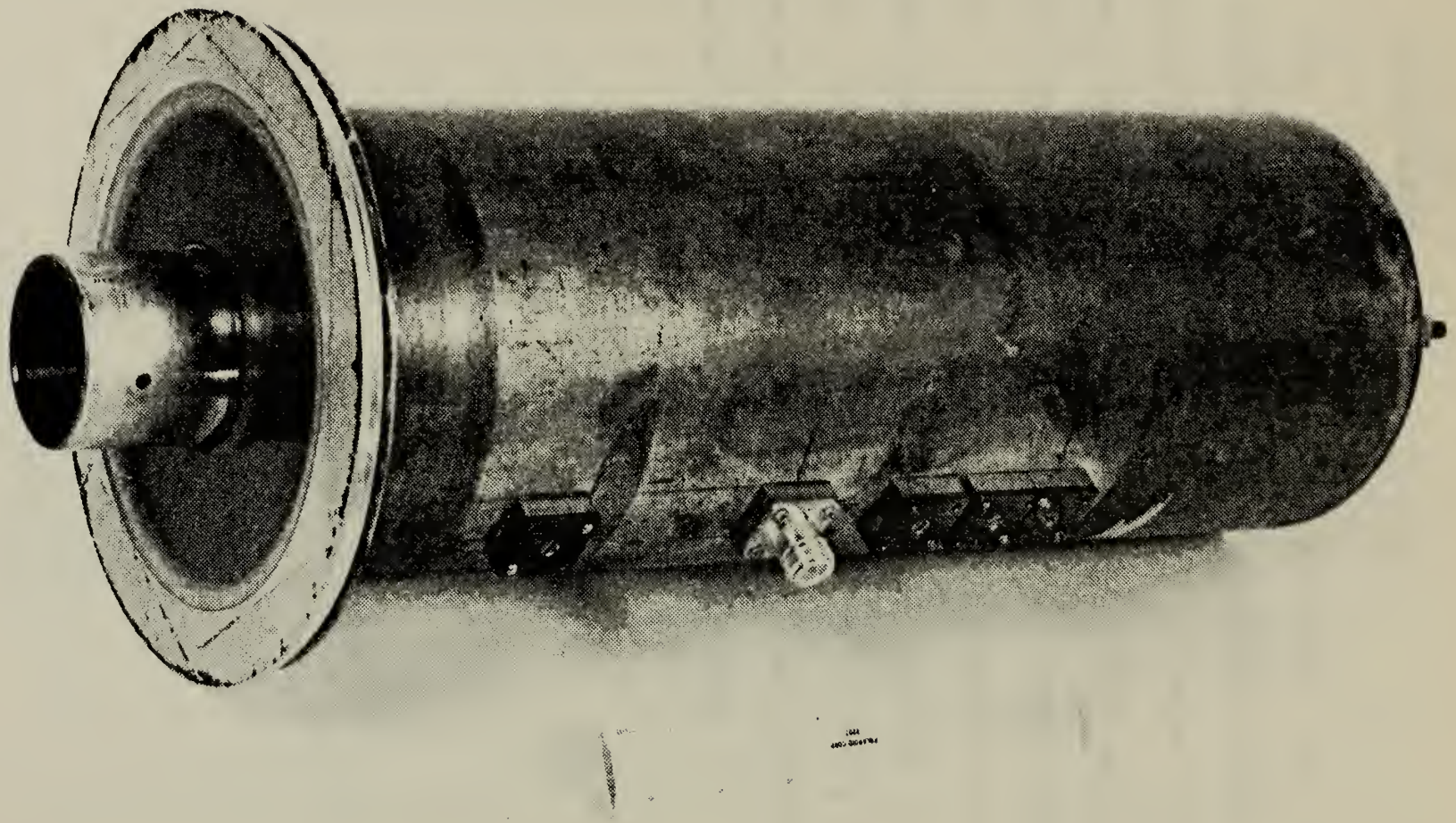

Figure 6. - Antenna feed system

3. Image Plane

The image plane (Figure 7) upon which the antennas were placed was a 10 meter square aluminum surface which formed the roof of an enclosure used to house equipment necessary for the antenna measurements. A 20.3 cm (8 inch) diameter circular opening in the image plane provided a location for mounting antennas. The flange at the top of the feed system fit into the opening, leaving a smooth surface atop the plane. The opening was located slightly off center on the square plane to reduce the possibility of resonances occuring on the image plane surface.

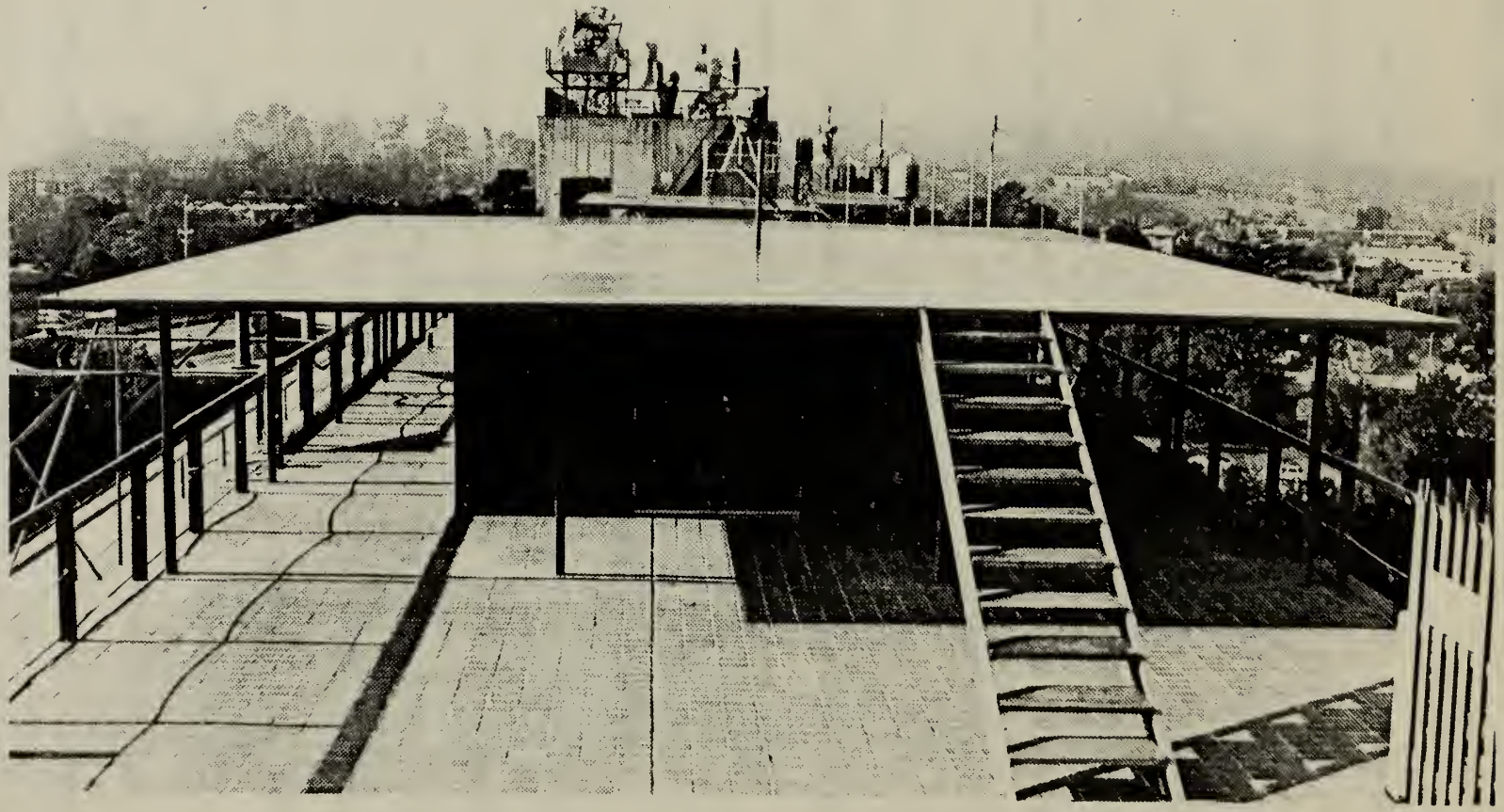

Figure 7. - Image plane structure

4. Charge and Current Probes

An accumulation of charge on a conductor is accompanied by an electric field proportional to the charge density. This electric field is perpendicular to the conductor surface for a perfect conductor and nearly perpendicular in the case of a very good conductor like brass. A monopole antenna oriented parallel to the electric field will therefore generate an EMF proportional to the charge density. If the monopole is small, it will react only to the charge density in the near vicinity and the probe's presence will have negligible effect on the field present. Similarly a wire loop positioned in a plane perpendicular to a changing magnetic field produced by an alternating current on the surface of a conductor will generate an EMF proportional to the time rate of change of current. As with the monopole probe, the loop must be small so as not to significantly disturb the current present on the conductor during the sampling process. For accurate resolution of current densities it must also be small so it is influenced only by currents in the near vicinity. For sinusoidal exitation the time rate of change of current is also sinusoidal so an EMF proportional to the current can be

obtained by applying a phase correction.

The principles discussed above were used in the design and construction of the charge and current probes (Figure 8) used to take experimental data on the crossed-monopoles. The charge probe consisted of a monopole antenna constructed from a section of Microdot Microminiature coaxial cable (250-3920). The outer conductor of the the coax was removed from a 17 mm segment of the cable to form the monopole probe which was mounted on the probe body. The teflon dielectric was left intact for added structural strength. The probe body was machined to fit into the .32 cm slots cut in the antennas so that the probe element was aligned perpendicular to the antenna surface. A beryllium copper retaining plate was used to hold the probe in place as it was positioned along the antenna. The center conductor of the coax was connected to a Microdot 31-34 connector which was made part of the probe body.

The current sensing element consisted of a semicircular section of UT-20 solid shield coaxial cable with .5 cm radius. The coax was terminated at one end on the probe body where a portion of the cable was hollowed out

and filled with solder. At the top to the semicircular arc a .5 mm gap was formed by removing the outer conductor and dielectric from the cable. The coax then continued intact through the semicircle and into the probe body where it was terminated at a Microdot 31-59 connector. The design and construction of the probes was based on previously established theoretical and experimental results [Whiteside 1962].

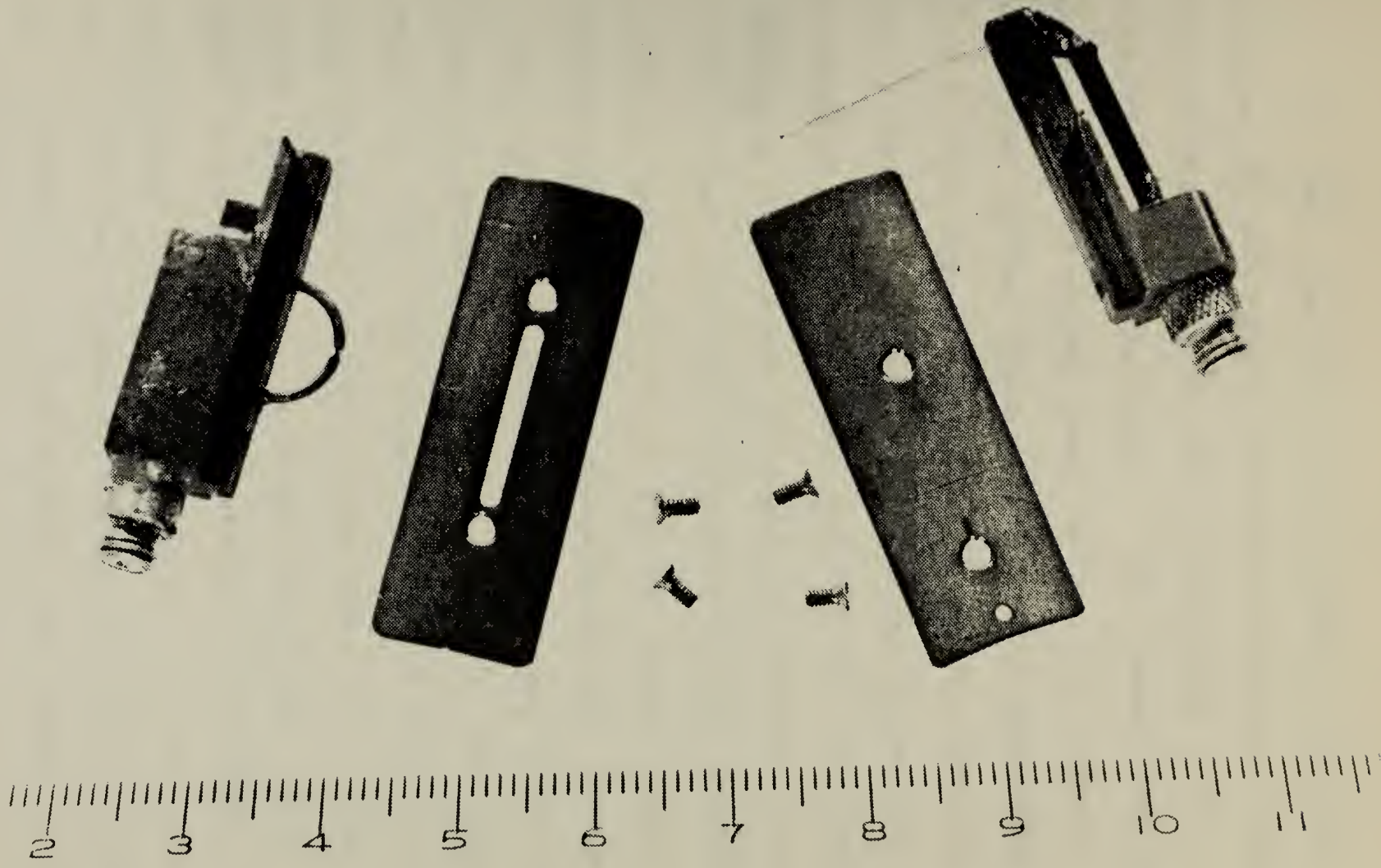

Figure 8. - Current and charge probes with retainer plates

The EMF generated by the probes provided an indication of the relative magnitude of charge and current density which was sufficient for the magnitude plots. To arrive at a true indication of the phase relationship between charge and current densities it was necessary to calibrate the probes. Phase calibration was accomplished by measuring the charge and current density distributions inside a coaxial feed systen similar to the one used to feed the antennas. The results were compared with distributions predicted by transmission line theory and correction factors were determined. The feed system used for probe calibration was 126 cm long and had a slotted center conductor to accomodate the probes. For a transmission line shorted at its end the voltage should lead the current by 90° within odd quarter wavelengths and lag by 90° within even quarter wavelengths. The data shown in Figures 9 and 10 depict charge and current density distributions at 195 Mhz and 300 Mhz respectively. A phase calibration factor was applied to the current data to establish the required phase relationships, +5.3° for 195 Mhz and +8.7° for 300 Mhz. These factors were applied to all antenna plots to provide a true representation to the phase relationships between distributions.

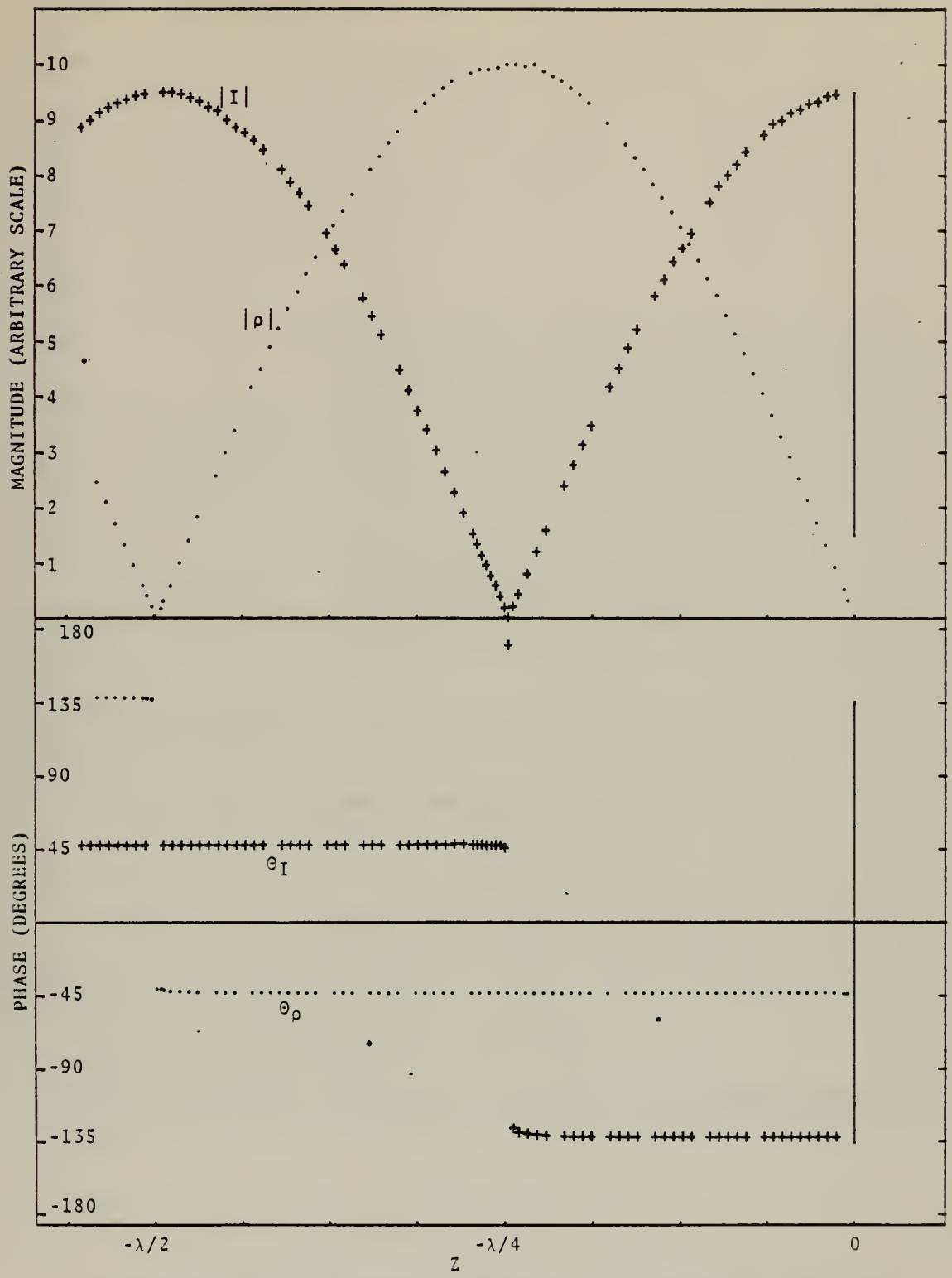

Figure 9. - Measured charge and current density distributions at 195 Mhz within a coaxial transmission line terminated in a short circuit

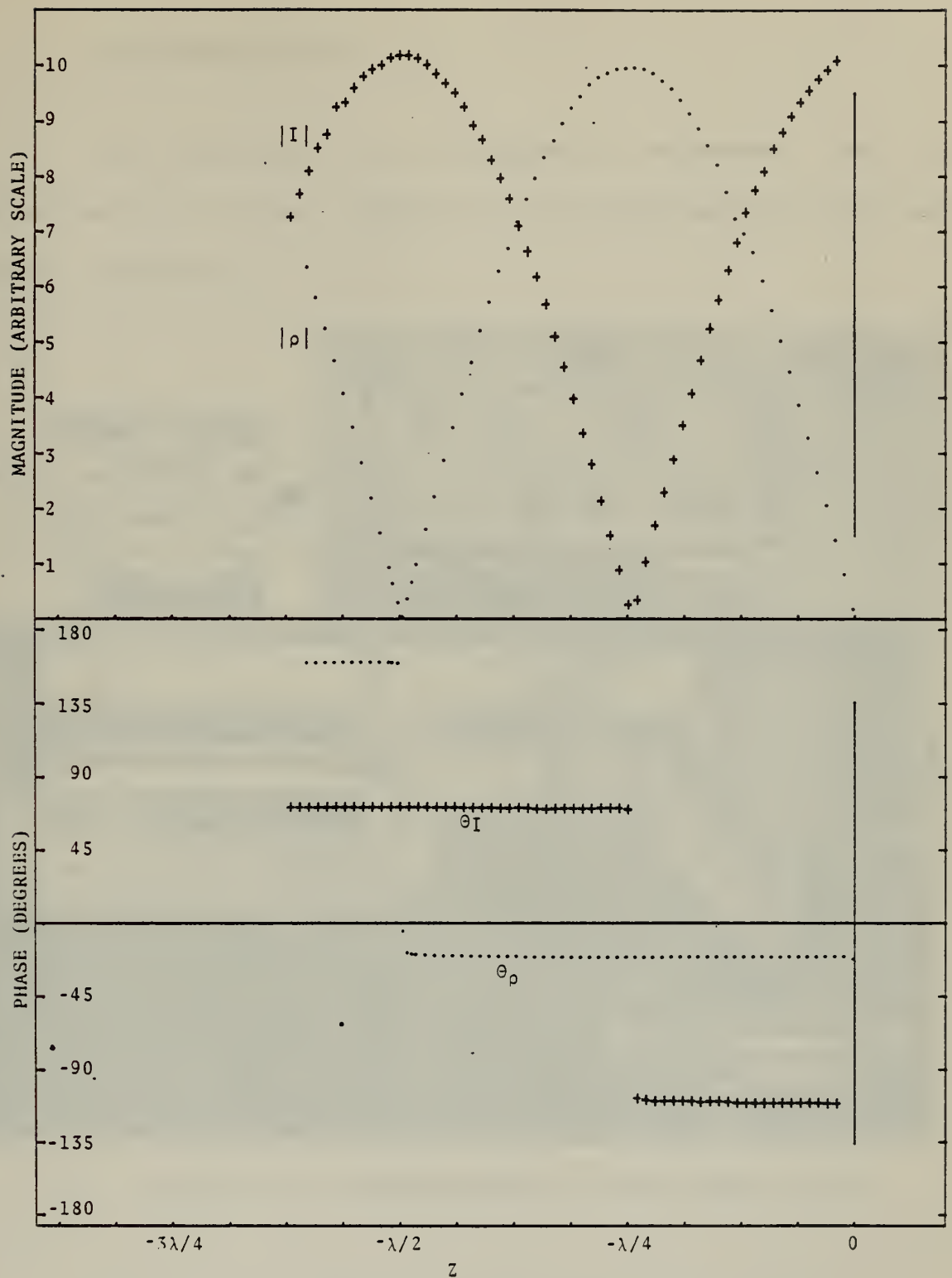

Figure 10. - Measured charge and current density distributions at 300 Mhz within a coaxial transmission line terminated in a short circuit

5. Instrumentation

The electronic test equipment necessary for the experimental set-up (Figure 11) was assembled from off the shelf components.

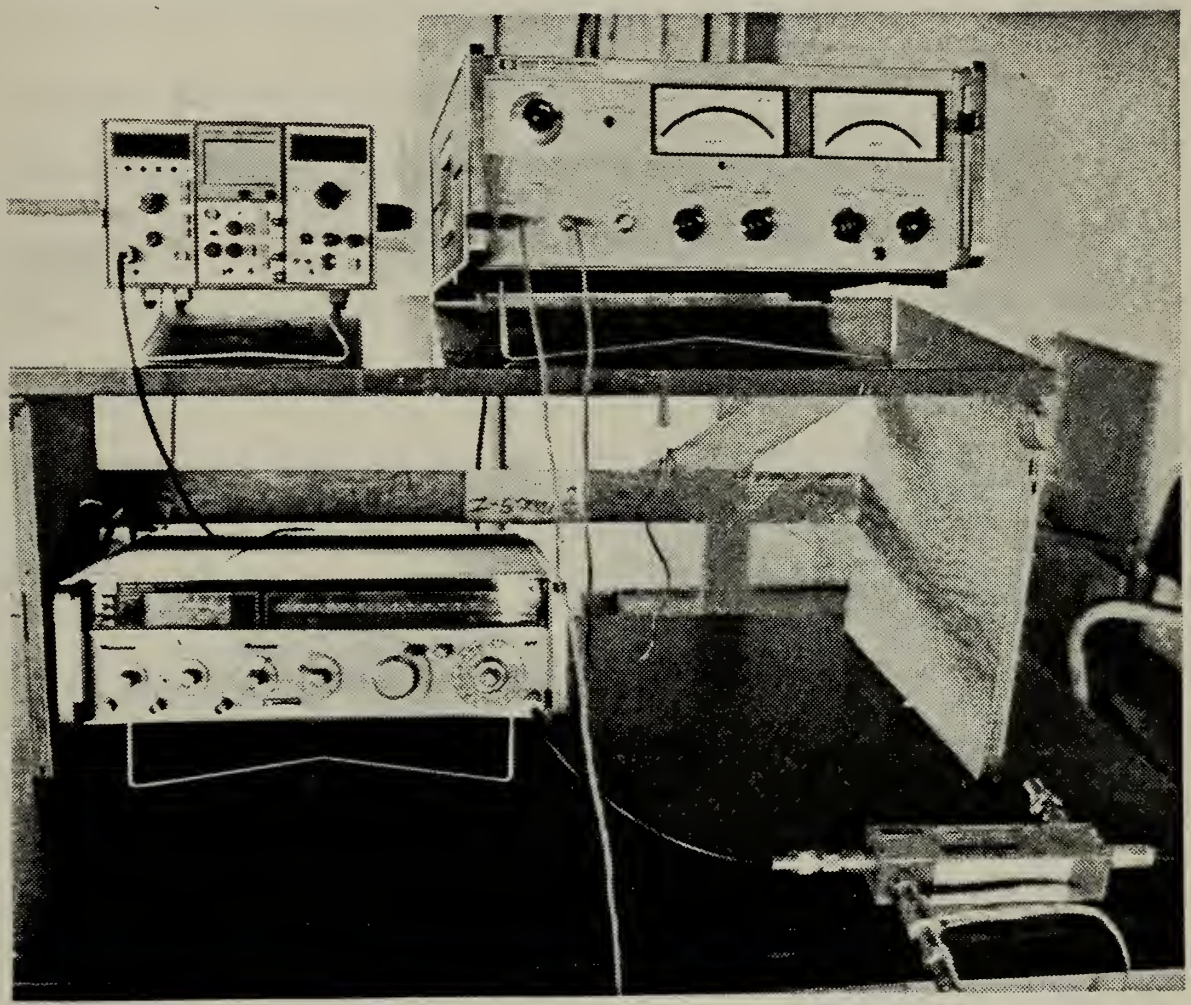

Figure 11. - Arrangement of instrumentation

Figure 12 shows the arrangement of test equipment in block diagram form. A Hewlett Packard 8640A signal generator was chosen to provide RF exitation for the antennas under test. The generator provided sufficient drive power (+20 dbm) to induce voltages well above the noise level in the charge and current probes. A reference output jack at the rear of the signal generator was fed to a Tektronix DC 502 frequency counter to monitor the output frequency. The signal generator was connected to a HP Model 764D dual directional coupler. The direct output of the directional coupler was divided by a HP 11549A power splitter and applied to the two N type connectors on the antenna feed system. The attenuated forward output from the directional coupler provided a sample of the drive signal for use in monitoring the power output. The power setting for all cases was maintained at +13 dbm at the direct output of the directional coupler. The directional coupler output representing a sample of the energy reflected from the antenna was not needed and was terminated with a HP 908A 50 ohm load. All interconnections were made with RG-8A or RG-9A coaxial cable. A Hewlett Packard 8405A Vector Voltmeter was used to measure amplitude and relative phase of the RF voltages induced in the charge and current probes.

A reference signal for the phase was applied to Channel A from the attenuated forward output of the directional coupler. The charge or current probe was connected to Channel B. Cables were adapted to the vector voltmeter probes with a HP 11536A 50 ohm tee and a HP 908A 50 ohm termination on each probe.

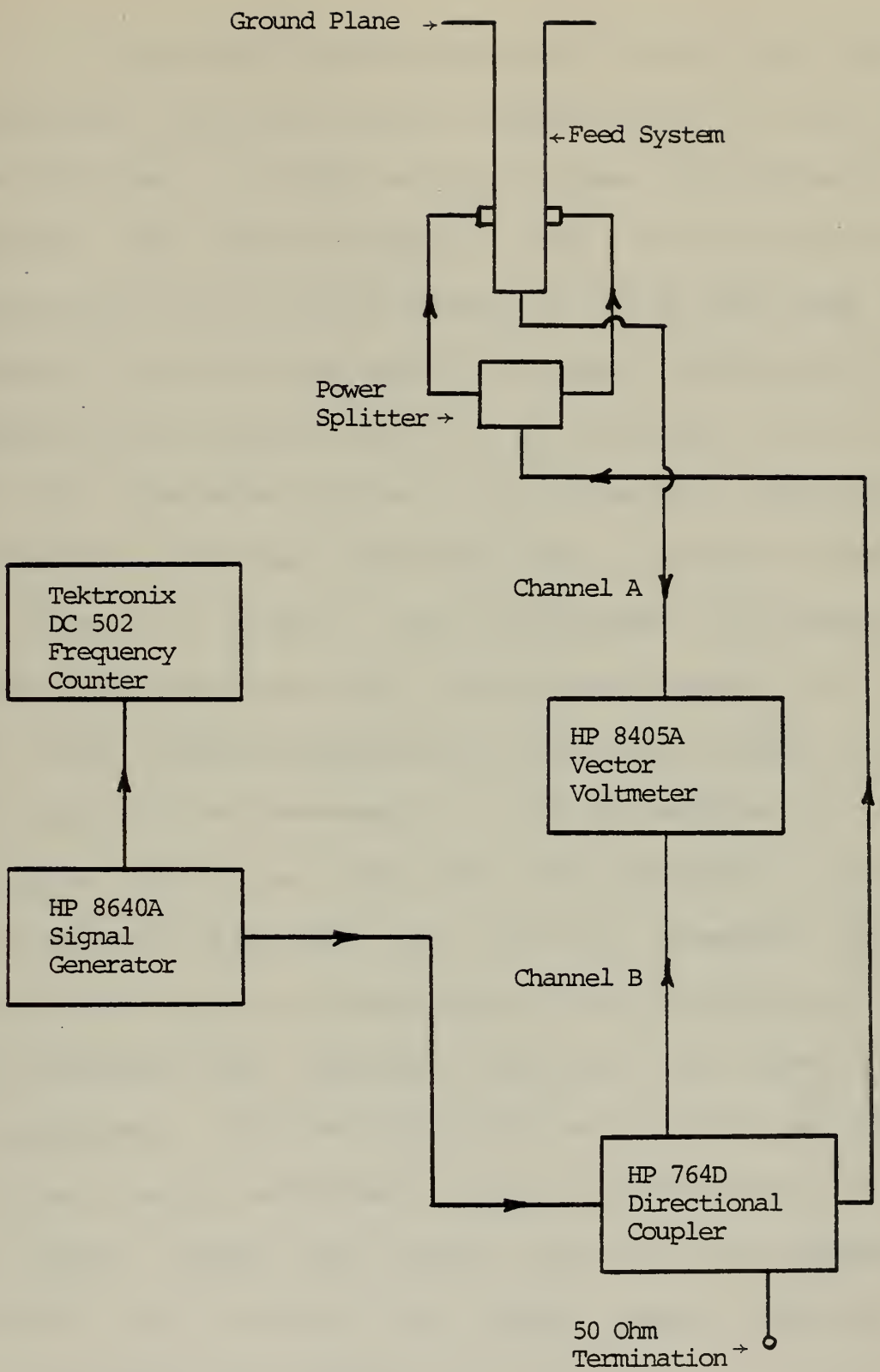

Figure 12. - Block diagram of instrumentation

A specially constructed coaxial cable was used to connect the charge and current probes, one at a time, to the test equipment. A rigid section of coax was constructed by removing the outer shielding from RG 142 B/U cable and inserting it into a 150 cm length of .32 cm (1/8 inch) brass tubing. At the lower end of the brass tube the RG 142 B/U continued with shield intact for an additional 190 cm were it was terminated with an N type connector. The upper end of the brass tube was terminated with a Mircodot connector to match the probes. This arrangement was adequate for positioning the probe along the vertical element. To allow for cross segment measurements a flexible section on top of the brass rod was necessary. A 42 cm section of double shielded cable was added for this purpose. To make all measurements compatible, the flexible extension was not removed for vertical measurements, thus no correction factor was necessary when comparing vertical and cross segment measurements. Additional shielding was found to be required for the flexible extension, it would otherwise pick up stray RF energy inside the antenna near the slot openings. A braided metal shield was added which reduced the interference significantly.

A rack and pinion positioning device (Figure 13) was fitted to the bottom of the feed system to move the charge and current probes along the antennas. The pinion gear was located in a movable housing which contained an index pointer, positioning knob, and provisions to fasten the rigid section of coaxial cable used for probe connections. The cable was drawn down as the positioning knob was turned, moving the probe along the antenna. The pointer indicated the relative position of the probe on a metric scale attached to the fixed rack.

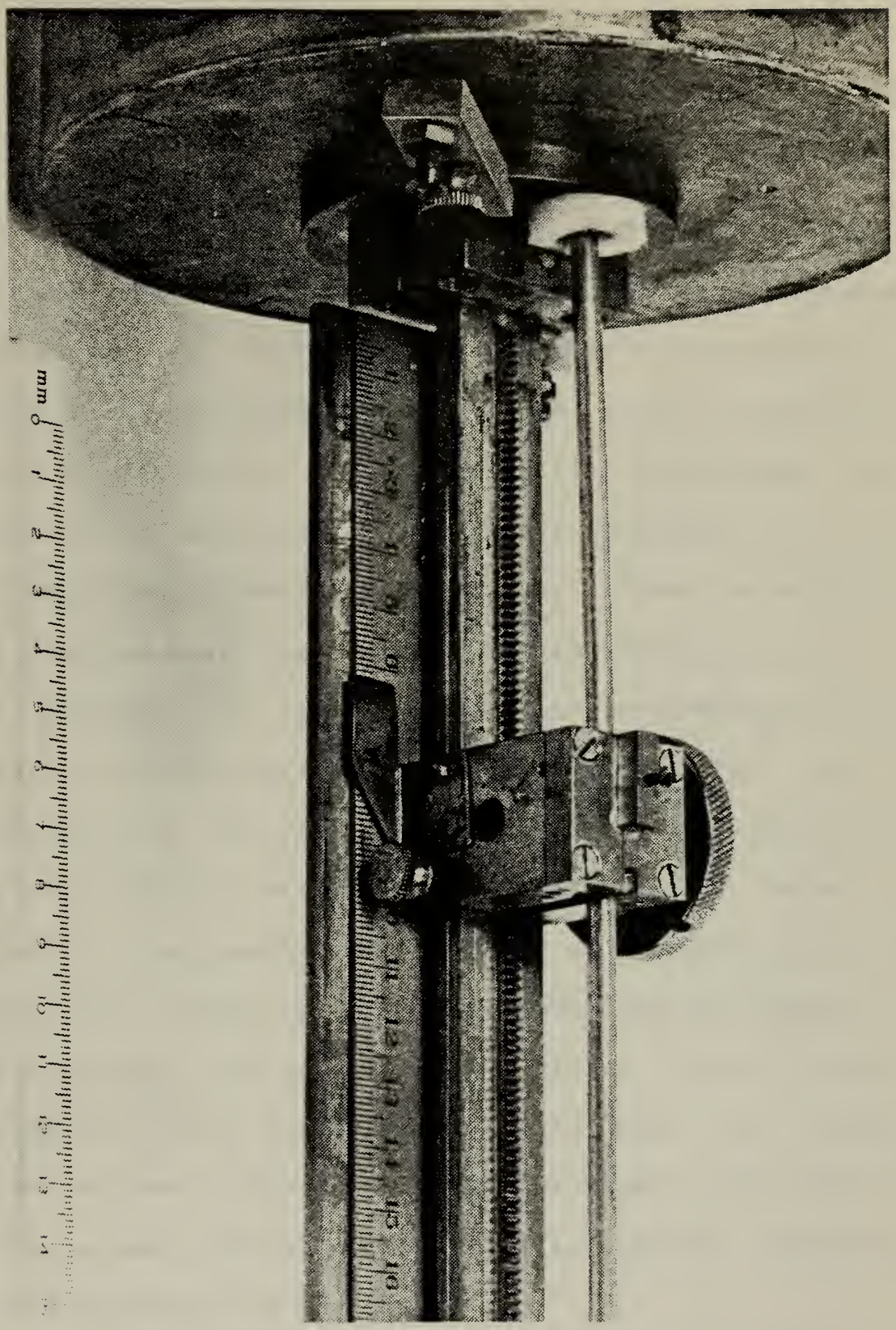

Figure 13. - Rack and pinion probe positioning mechanism

B. EXPERIMENTAL PROCEDURE

1. Antenna Configurations

The electrical length of the crossed-monopole antennas were manipulated to produce four configurations. The intent was to locate the junction at the position of different combinations of maximum and minimum charge and current densities. The different configurations were obtained by adjusting the physical dimensions of the antennas and the excitation frequency. Since the height of the junction above the ground plane was fixed at 68.5 cm it was necessary to vary the excitation frequency until the chosen conditions were satisfied. The total height of all configurations was fixed at 137 cm to place the junction at the center of the vertical member maintaining a degree of symmetry. Experimental data on a 137 cm monopole at 300 Mhz (Figure 14) places a charge minimum/current maximum at approximately 68.5 cm from the ground plane. An ideal treatment of this configuration would place the minimum charge/maximum current 75 cm (3/4 wavelength) from the top of the antenna but end effects cause an apparent shortening of the wavelength on the antenna.

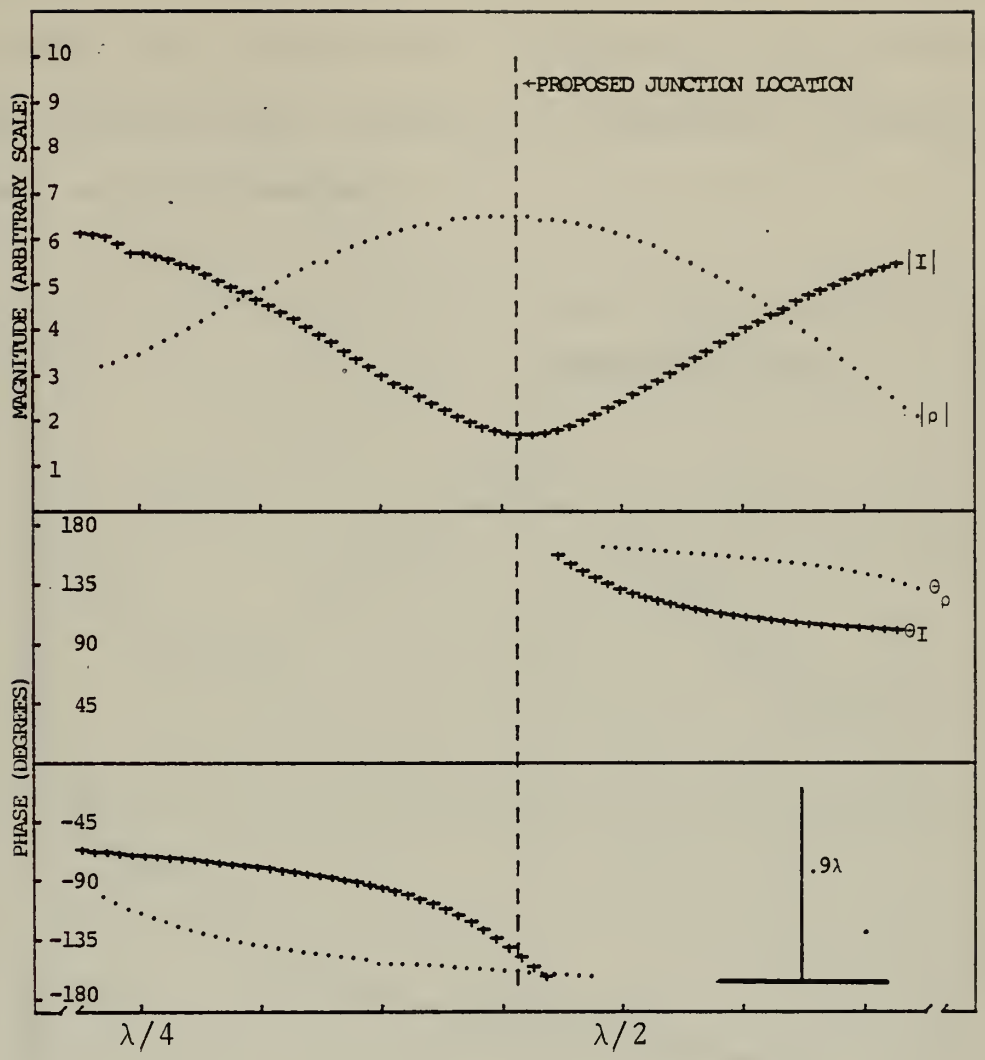

Figure 14. - Measured charge and current density distributions on the reference monopole at 195 Mhz

The frequency required to place a charge maximum/current minimum on the monopole 68.5 cm above the ground plane was 195 Mhz (Figure 15). The physical length of the cross arm segments required to reflect a particular charge and current condition was derived from the experimentally determined

distances for the monopole. The four cases tested are depicted in Figures 17, 20, 23 and 26. Each figure illustrates the zeroth-order solutions for the charge and current distributions, assuming no interaction between the vertical and cross members.

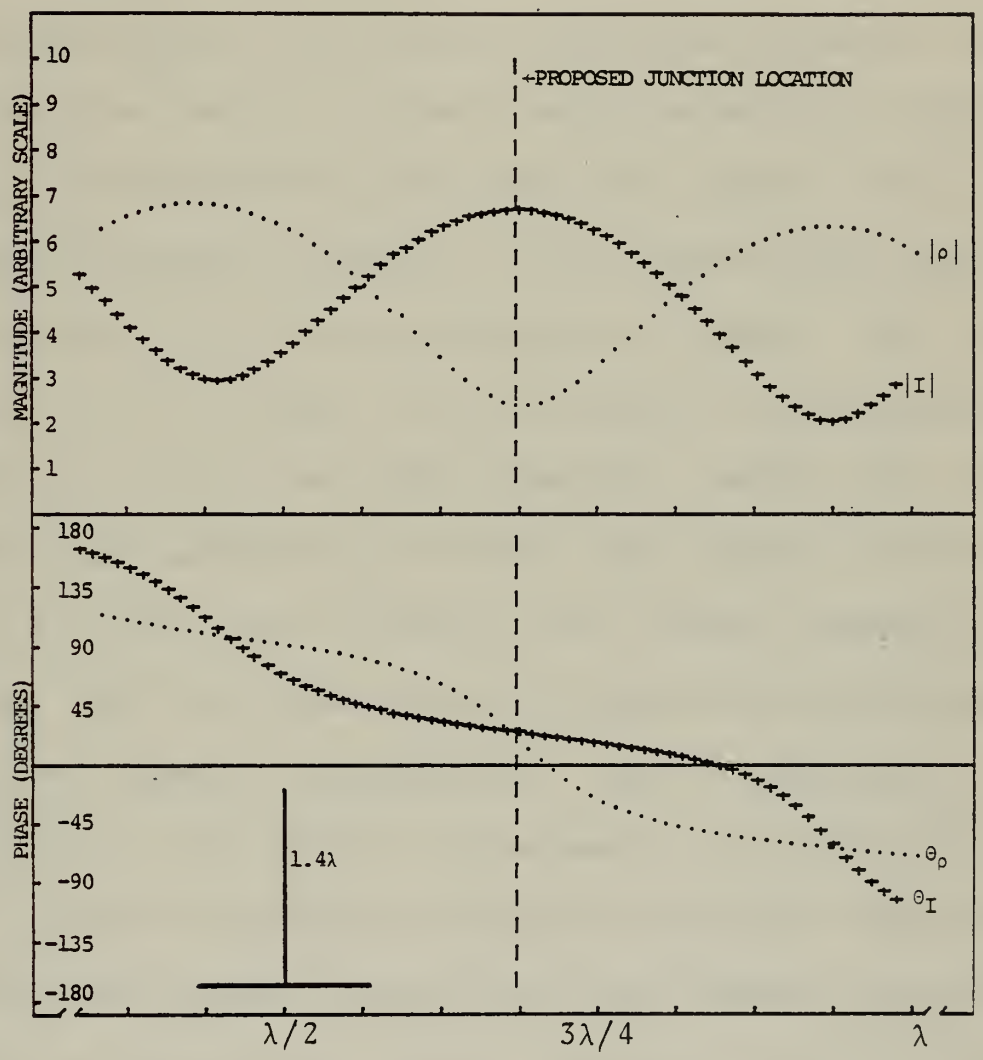

Figure 15. - Measured charge and current density distributions on the reference monopole at 300 Mhz

2. Data Acquisition

Data was taken at 1 cm increments along the antenna segments, or approximately every .01 wavelength at 300 Mhz, .0065 wavelength at 195 Mhz. At each position the magnitude and relative phase of the probe voltage was recorded. Each data run was begun by positioning the charge or current probe at the furthermost point from the antenna base and locking the pinion housing on the brass tubing with the index mark at 0 cm on the attached metric scale. The true position of the probe on the antenna was recorded to correlate it with the scale readings beside the rack. Positions were measured up from the image plane. At the end of each run the actual position was again measured and compared with the index reading to check for any slippage. For cross segment measurements some inaccuracy was introduced by the pulley arrangement. As tension on the pulley varied the pulley was displaced slightly to the side, degrading the agreement between the scale reading and actual position on the antenna. Errors detected did not exceed ±.15 cm (.0015 wavelength at 300 Mhz, .0007 wavelength at 195 Mhz).

The vector voltmeter was checked and calibrated immediately before data acquisition started. Its accuracy was ±6% of full scale for the voltage readings and ±4.5° for phase measurements. The vector voltmeter was capable of phase accuracy of ±1.5° if both channels received the same amplitude signal but it was impractical to readjust the signal applied to the reference channel for every data point.

3. Data Processing

A Hewlett Packard 9821A Calculator and 9862A Plotter (Figure 16) were used to process and display all data. Two programs were utilized to perform the necessary operations. Appendix A includes a listing of both programs. One program provided a means of storing on magnetic tape the charge and current data along with parameters identifying the configuration. A second program processed the data and plotted it. Processing included converting the scale readings along the rack and pinion assembly to true positions along the antenna, scaling for graph plotting and converting physical measurements to fractions of a wavelength.

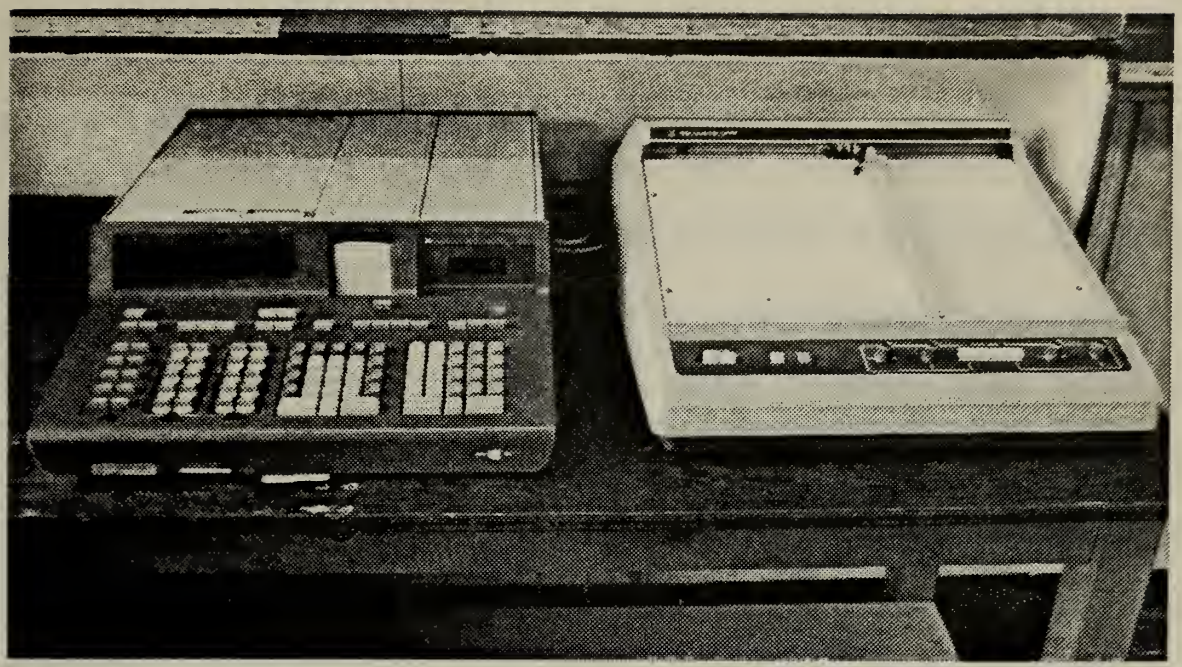

Figure 16. - Data processing equipment

4. Data Analysis

Analysis of the charge distributions on the crossed-monopoles was a straightforward proceeding. The magnitude and phase varied sinusoidually with only minor variations for all cases. Comparison with data from the reference monopole and with theoretically predicted distributions could be carried out directly. Assuming an ideal point junction, a boundary condition could be imposed requiring that the amplitude and phase of charge along all segments converge to a common value at the junction [Burton

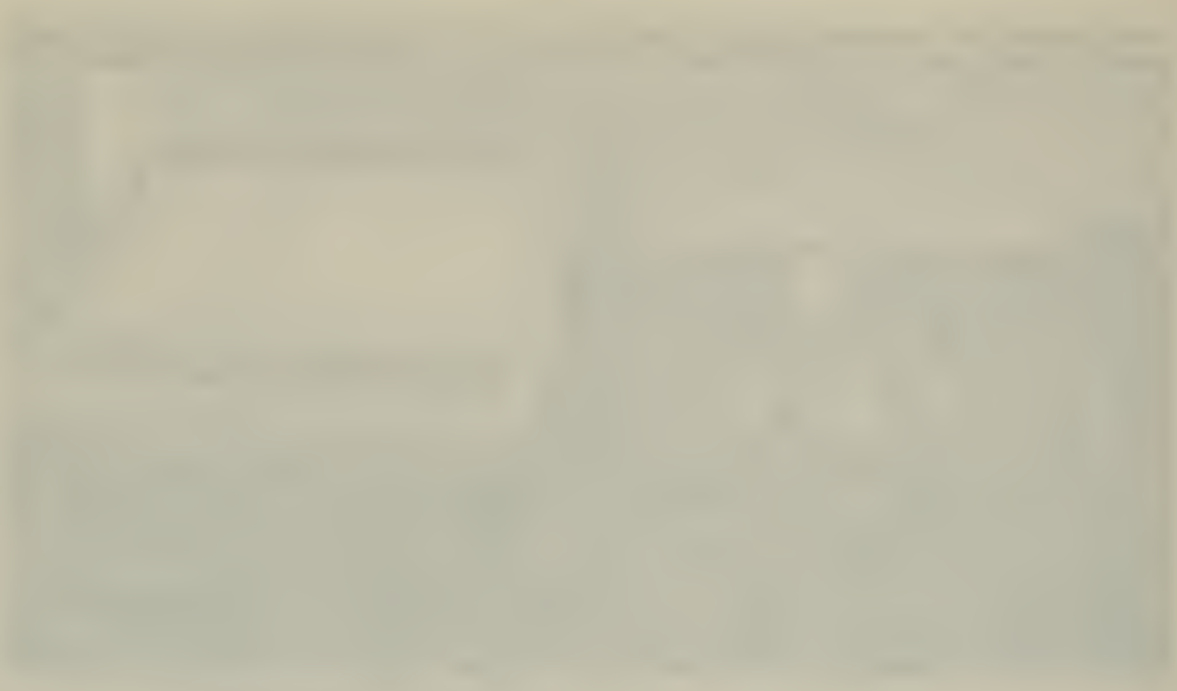

and King 1975]. Extrapolation of the data presented confirms this fact in each of the four cases.

Kirchoff's Current Law, that the vector sum of currents entering a junction sum to zero, may be applied to the cross junction. Unfortunately, mechanical limitations prevented taking cross arm data closer than within approximately 6 cm of the junction and the vertical current data suffers some inaccuracy near the junction center. As the probe approaches to within a few centimeters of the junction center an abrupt change in the current magnitude data occurs just as the retaining plate bridges the gap formed by the intersecting slot from the cross arm. After the probe has passed through the junction center the retaining plate passes over the gap and from that point on the data is free from irregularities. Even if precise data was available at the junction it would be inadequate for application of Kirchoff's Law since the probe would be sensitive to currents flowing only along the two axes of probe orientation while at the junction center current may be flowing in any direction. A practical solution would be to move back from the junction a short distance along all four segments where it could be assumed that the currents still possess rotational symmetry and are predominantly

flowing longitudinally. A distance twice the radius of the antenna away from the junction center was chosen as the location to take data for application of Kirchoff's Current Law. This distance (6.35 cm) is approximately the point where the cross data starts, it is beyond the irregularity caused by the probe retainer plate, and is not so far from the junction so as to introduce any significant error due to displacement from the junction where Kirchoff's Law should theoretically be applied.

a. Case 1

The vertical member standing alone as a monopole would support a standing wave pattern with a maximum current/minimum charge at the position of the junction. The two cross segments are each one half wavelength suggesting that the boundary conditions at the cross segment ends would normally reflect a current minimum a half wavelength back, at the junction (Figure 17).

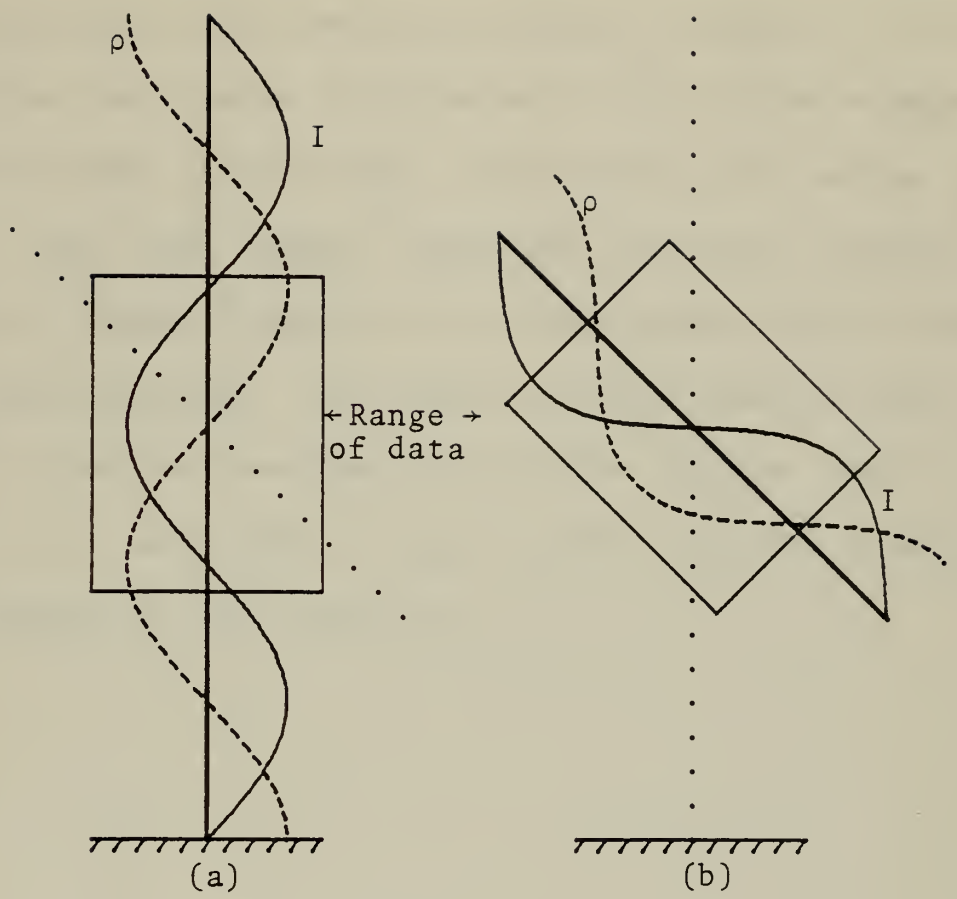

Figure 17. - Assumed charge and current density distributions for Case 1 crossed-monopole

Comparing the charge distributions on the ideal crossed-monopole vertical member current shown in Figure 18 with the zercth-order distribution shown in Figure 17 it may be seen that the charge distribution on the crossed-monopole retains the same general shape and locations for maxima and minima. The peak charge magnitude above the junction is reduced, an expected result due to the loading effect caused by the cross segments. The junction charge density does not achieve a lower minimum due to the effect of the cross arm which is an electrical length which reflects a maximum charge density at the junction.

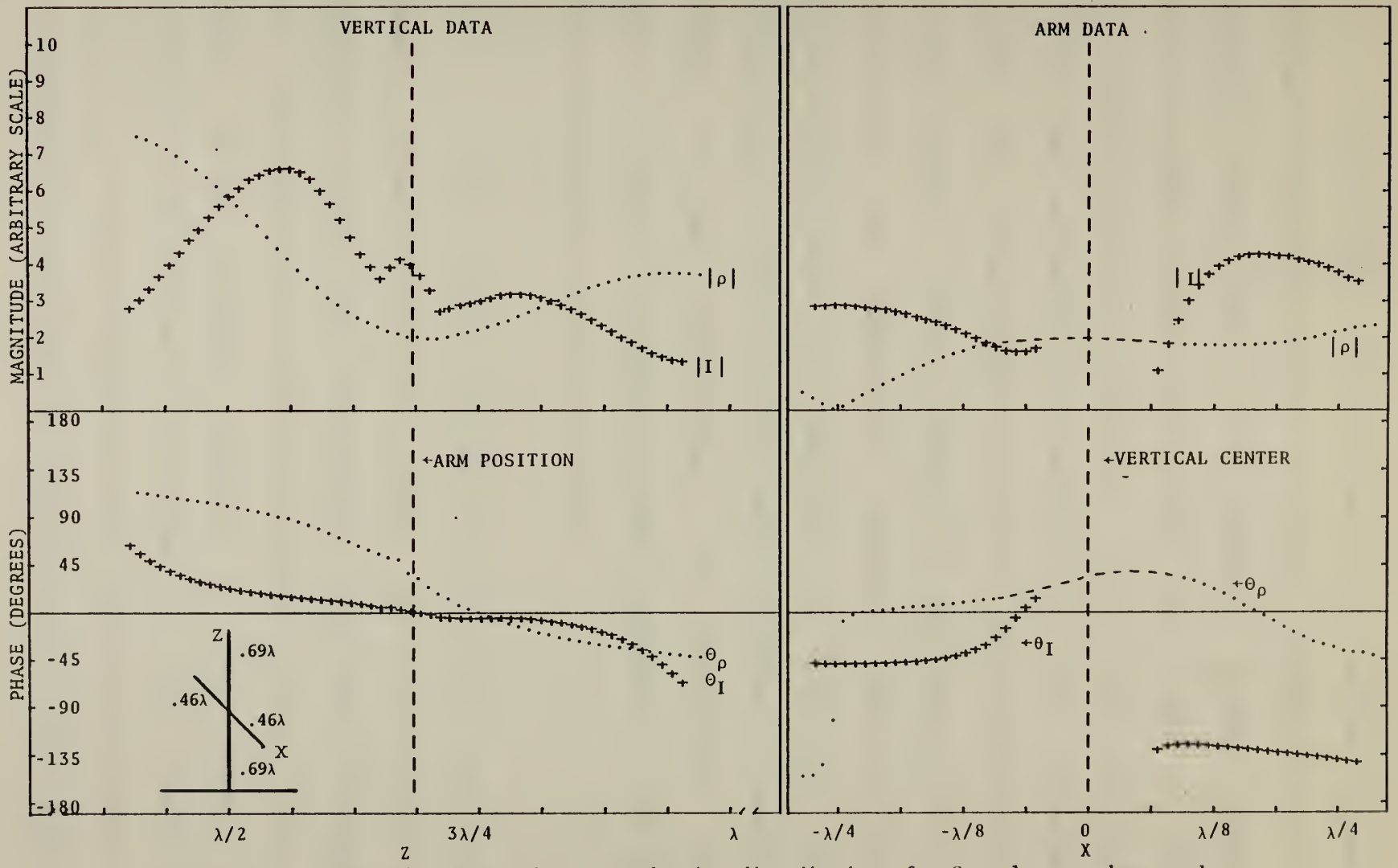

Figure 18. - Measured charge and current density distributions for Case 1 crossed-monopole

The current distribution on the vertical element maintains a sinusoidal pattern to within approximately 1/8 wavelength either side of the junction. Minimum current magnitudes appear to occur just beyond the range of data both above and below the junction. If so, their occurrence is near the corresponding positions on the reference monopole, but in each case displaced a short distance away from the junction. This is contrary to the results for the perpendicular case studied by McDowell, where the lower minimum occured nearer the junction; an indication that impedance seen at the feed point could be varied by changing the angle of cross intersection. An intermediate point could be chosen to present the same impedance at the feed point as a monopole of the same height.

The charge concentrations along the cross segments apprcach a relative maximum at the junction as presupposed using the zeroth-order approximation (Figure 17b). The same point is a relative minimum for the vertical member, so the natural condition on both members is satisfied. A dashed line on the cross arm data near the junction in Figure 18 indicates the assumed convergence of the magnitude and phase of the charge density. The value at

the center of the cross arm was taken as identically the same as that recorded on the vertical member at that same position, which it in fact must be. It is reasonable to assume that no radical variations in charge density occur in the short distance where data was unavailable. All four cases were treated in this manner. The upper cross arm presents an approximately sinusoidal distribution for charge with a minimum occuring 1/4 wavelength from the junction. The current is likewise sinusoidal with a maximum at 1/4 wavelength. Both distributions seem little disturbed by their proximity to the upper vertical element. The lower cross arm is, however, a different matter. The larger concentration of charge and greater magnitude current disturb the natural resonance of the arm. Where a minimum charge would be expected about 1/4 wavelength from the junction the charge magnitude is still increasing under the effect of the concentration of opposite polarity along the lower vertical element. The phase relationship between arm and vertical segments provides another indication of the interaction which occurs between cross segments. Below the junction the charge concentration can be assigned a polarity, say positive, for reference. Figure 18 depicts the phase in the region of maximum charge concentration to be approximately +130°. On the lower cross arm segment

adjacent to this charge concentration the phase of the maximum charge is approximately -45°, nearly 180° out of phase with the vertical member charge. The current plot is likewise distorted under the influence of the adjacent vertical element. The current maximun 1/8 wavelength below the junction is located directly across from the position of the disproportionately high current maximum on the lower cross arm as a result of inductive coupling.

It is not apparent from observing the data in Figure 19 that Kirchoff's Current Law is satisfied at the junction. a vector diagram showing the sum of currents existing 6.35 cm from the junction center (Figure 19) demonstrates that the currents at that point approximately add to zero. An exact cancellation is unlikely since the currents chosen only approximate those at the junction, approximately 1/16 wavelength away. The vectors shown include 180° corrections where necessary to account for the probe sensing direction.

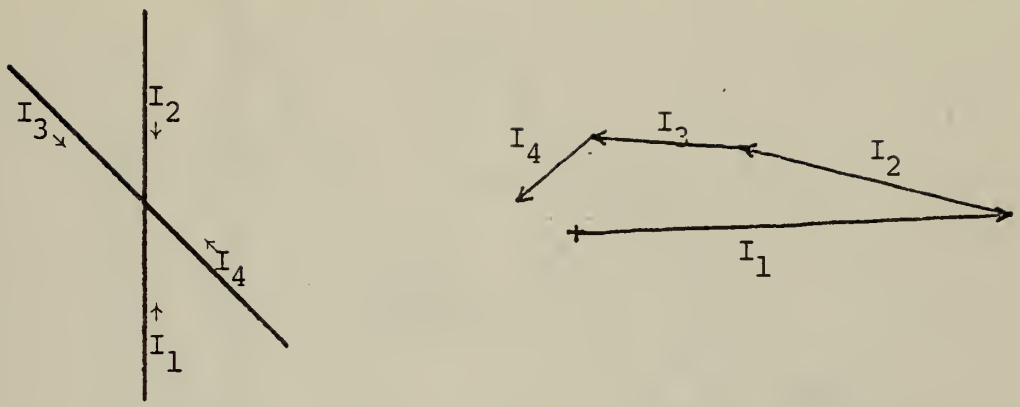

Figure 19. - Application of Kirchoff's Current Law at junction of Case 1 crossed-monopole

b. Case 2

This case combines the vertical and cross segments in a more compatible, or reinforcing, combination of natural resonances. In this instance all segments are of equal length. The vertical member standing alone (Figure 20a) would present a maximum current/minimum charge at the junction. The cross segment lengths alone (Figure 20b) would also reflect a current maximum/charge minimum at the junction.

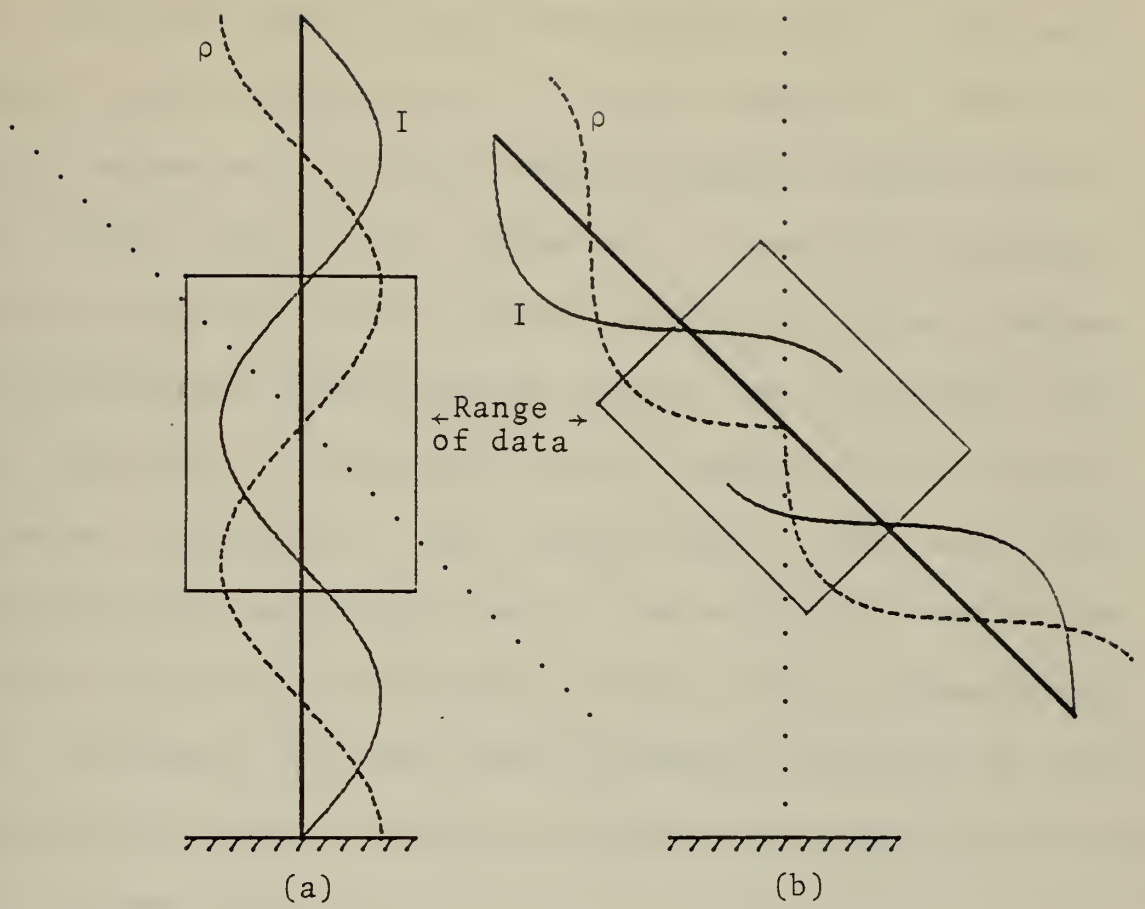

Figure 20. - Assumed charge and current density distributions for Case 2 crossed-monopole

The data from the vertical member of the cross (Figure 21) is nearly the same as that recorded for Case 1. The charge minimum at the junction has a lower magnitude since the cross elements are also tending toward a charge minimum. The upper cross arm supports a smooth sinusoidal distribution for both charge and current with a minimum current/maximum charge located nearly 1/4 wavelength from the junction, a situation which agrees with the natural resonant conditions. The lower cross arm also has distributions much like Case 1. The similarity between the lower cross arm distributions on Cases 1 and 2 suggests that the influence of the lower vertical element is more significant than arm length in deciding the distributions on the adjacent cross arm.

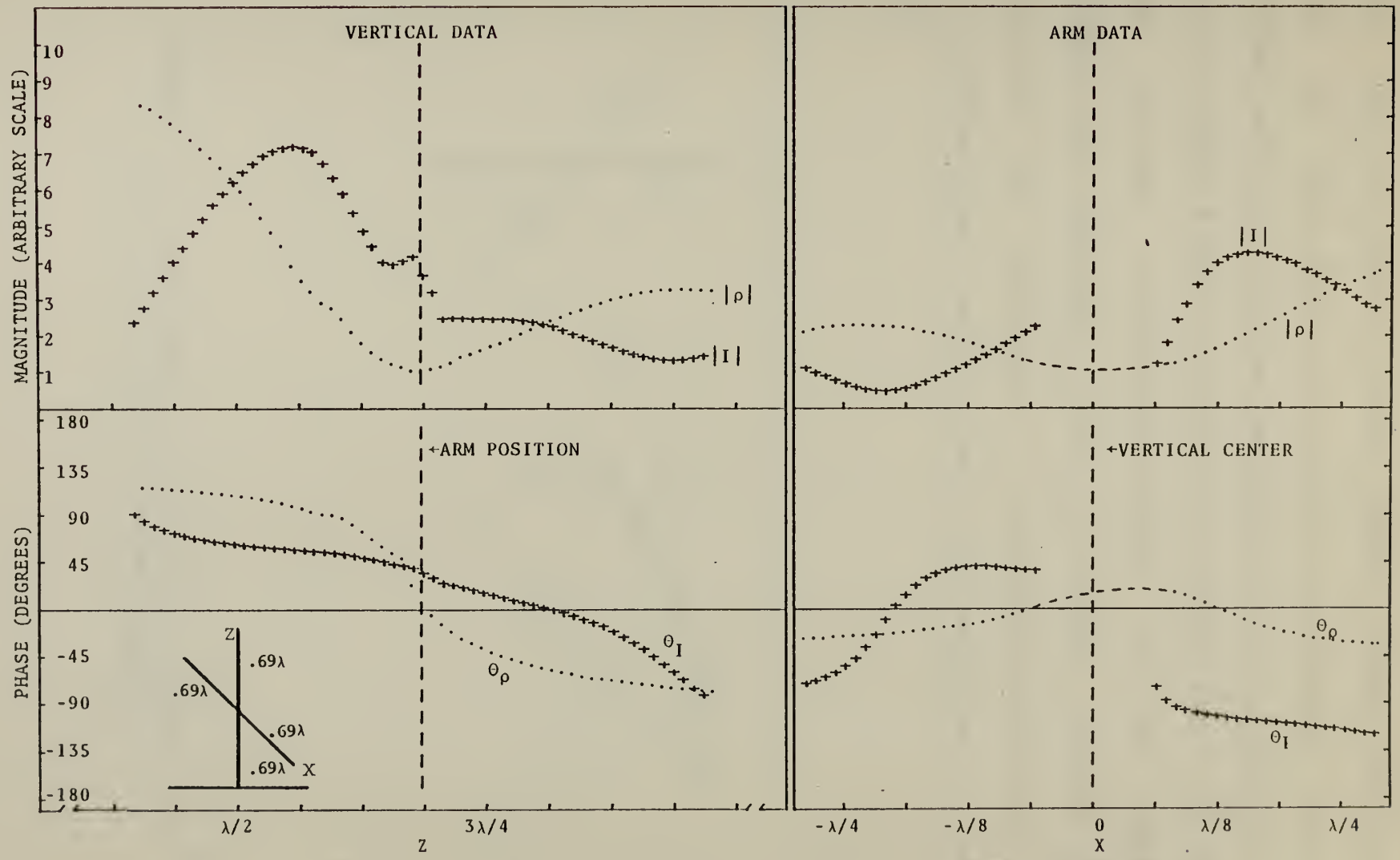

Figure 21. - Measured charge and current density distributions for Case 2 crossed-monopole

In Case 2 the resulting distributions have higher magnitude since there is closer agreement between natural and forced modes. The charge density recorded at the junction on the vertical data plot compares favorably with the magnitude and phase of charge density arrived at by extrapolation of the cross arm data. The vector addition of the currents recorded 1/16 wavelength from the junction (Figure 22) illustrates the application of Kirchoff's Current Law to this configuration. As with Case 1, the vector sum is near zero.

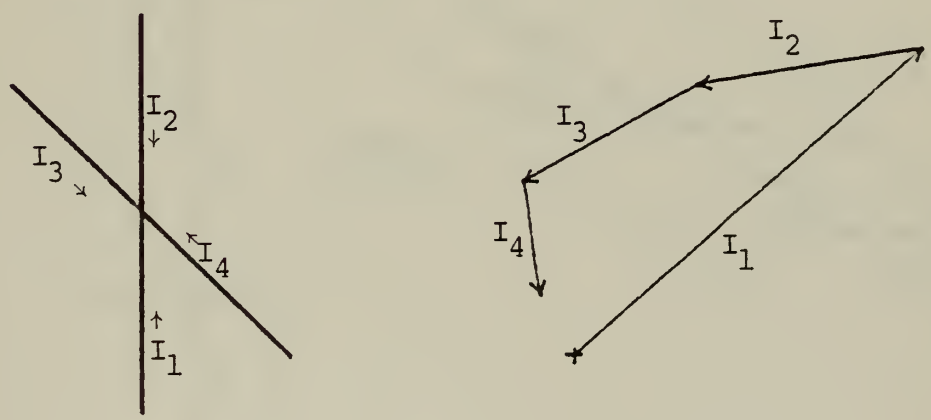

Figure 22. - Application of Kirchoff's Current Law at junction of Case 2 crossed-monopole

c. Case 3

This configuration was constructed with four equal segments, each 1/2 wavelength long. The resonant modes of each place a maximum charge/minimum current at the junction (Figure 23).

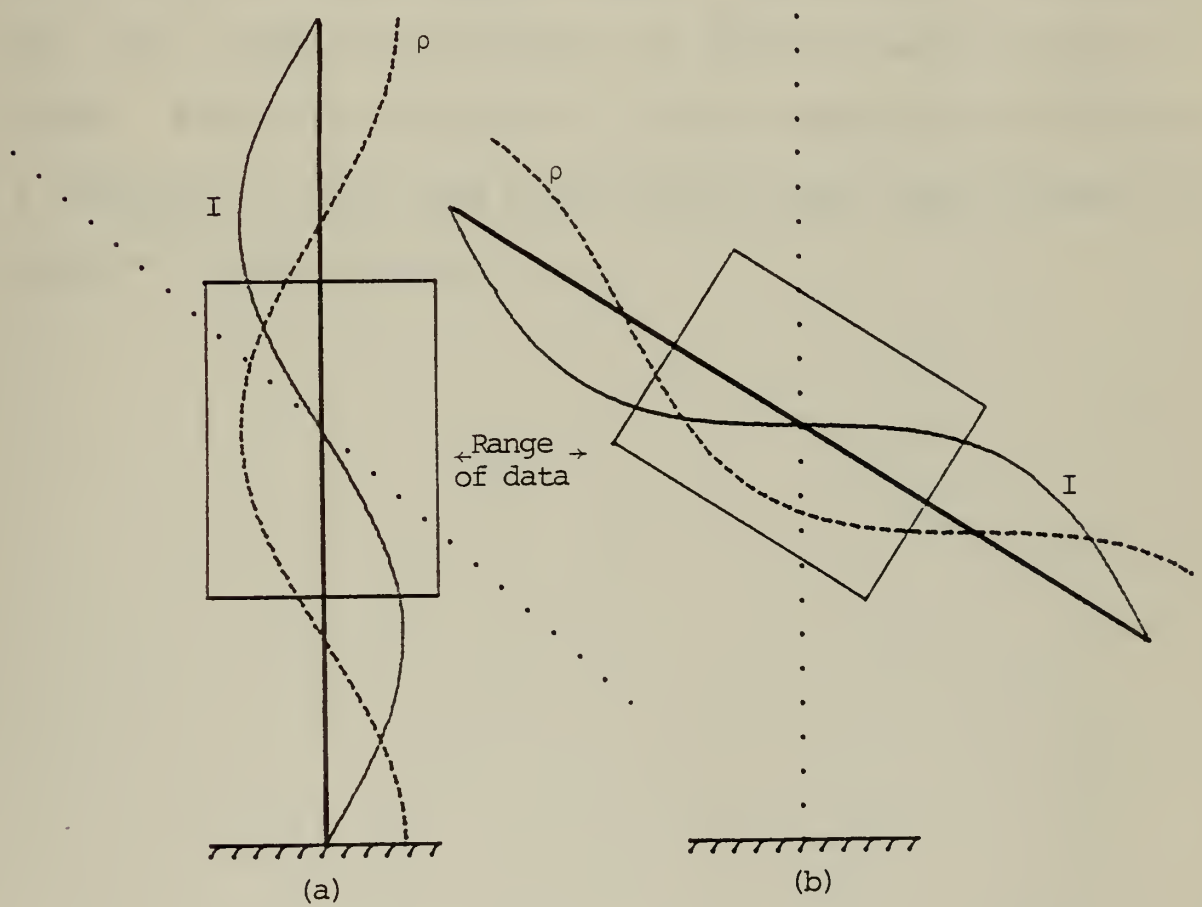

Figure 23. - Assumed charge and current density distributions for Case 3 crossed-monopole

The data recorded for the cross (Figure 24) indicates a relative charge maximum for three segments at the junction, a relative minimum for the lower vertical element. The vertical member distributions depart significantly from the ideal case (Figure 23a). The charge density is monotonically decreasing across the entire range of data with a minimum at the topmost data point on the antenna. The vertical member current density distribution maintains the same general shape below the junction as the first two cases. Above the junction the current density climbs toward a maximum in the same manner as the ideal case, though it appears to peak earlier.

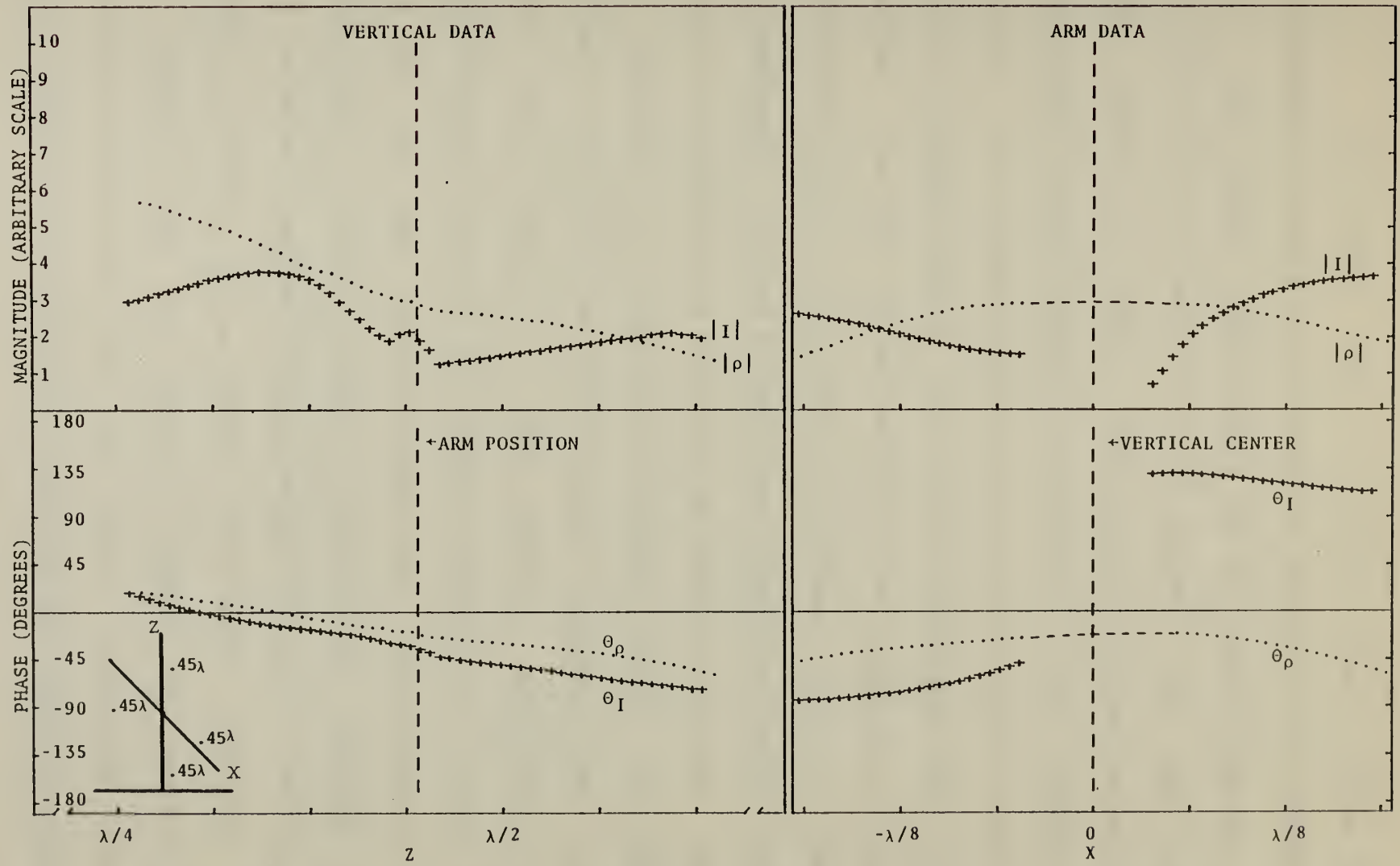

Figure 24. - Measured charge and current density distributions for Case 3 crossed-monopole

As with Case 2, the upper cross arm distributions closely approximate the expected plots (Figure 23b). The charge distribution on the lower cross arm is also much like the ideal case and matches the upper arm almost point for point. The current distribution on the lower cross arm again shows the effects of the inductive coupling. The current standing wave on the vertical member reaches a maximum between 1/16 and 1/8 wavelength below the junction. As the current builds in one direction, falls, and builds again in the opposite direction a varying H field is generated. As the H field cuts across the nearby lower cross arm, currents are generated as would be the case when any conductor is present in a varying H field. The close proximity and greater magnitude current combine to make the effects more noticable at this location. Regretably, the lower frequency required for scaling resulted in a range of data for the arms which was less than 1/4 wavelength. A trend toward a current maximum is nevertheless apparent on both arms and a sinusoidal progression toward the end point boundary condition can be assumed. The vector addition of the currents near the junction (Figure 25) was not as successful as with the first two cases. Undetected rapid phase shifts in arm currents very near the junction render

the samples invalid for application of Kirchoff's Law at the junction. In the first two cases the current phase exhibits no radical changes near the junction, lending credibility to the approximation technique. In this case a phase shift of almost 180° occurs within 1/16 wavelength of the junction above the vertical element and a steep slope is apparent on the lower cross arm current phase at the end of the data.

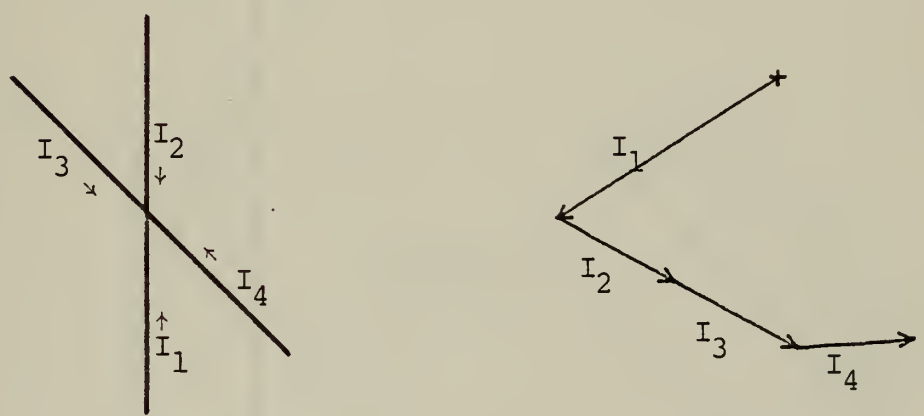

Figure 25. - Application of Kirchoff's Current Law at junction of Case 3 crossed-monopole

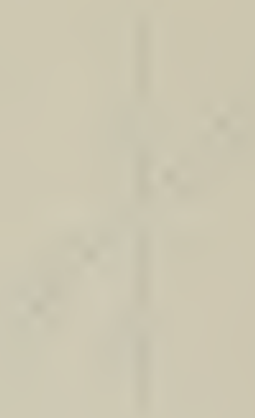

d. Case 4

This configuration shows the most radical departure from the expected resonant mode for the vertical member (Figure 26a). As with the other three cases, the current magnitude records a peak just below the junction center (Figure 27).

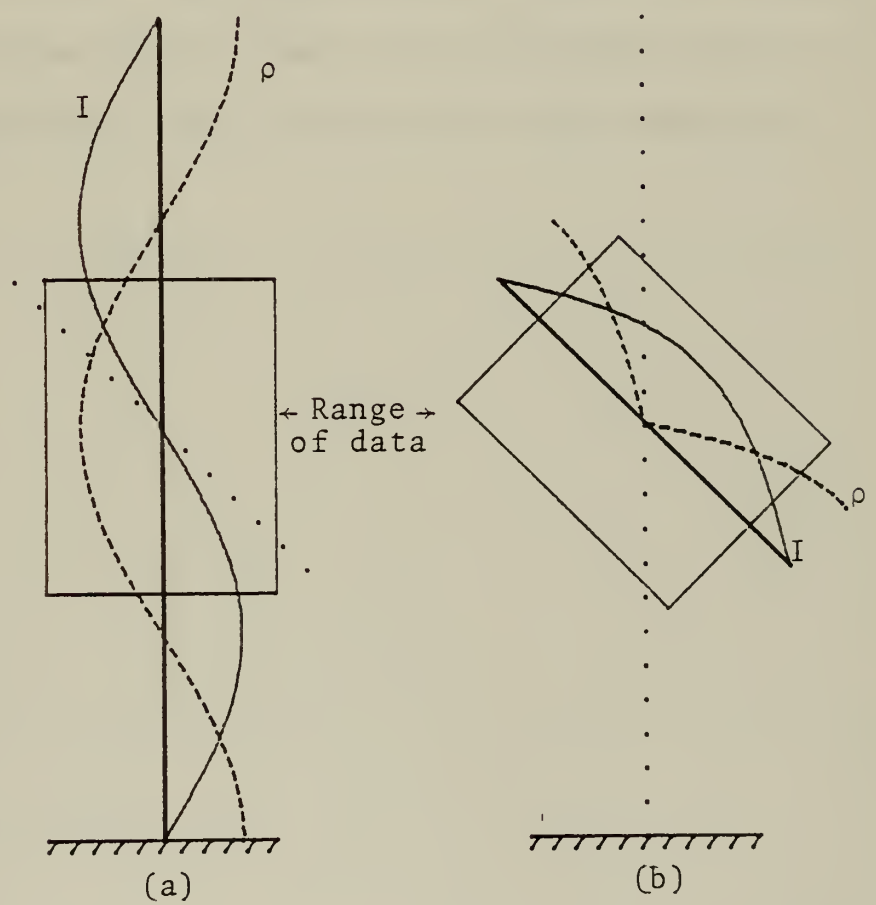

Figure 26. - Assumed charge and current density distributions for Case 4 crossed-monopole

Just above the junction a sharp minimum occurs accompanied by a rapid 180° phase shift. Further above the junction the current tends toward a maximum that presumably occurs near 1/4 wavelength above the junction. The vertical charge distribution is likewise markedly different than expected. Although a charge maximum was predicted at the junction, a charge minimum occurs very near the junction along with a 180° phase shift. The magnitude of the arm exitation is largest of any of the cases, and the upper arm has a larger current magnitude than the lower for this case alone.

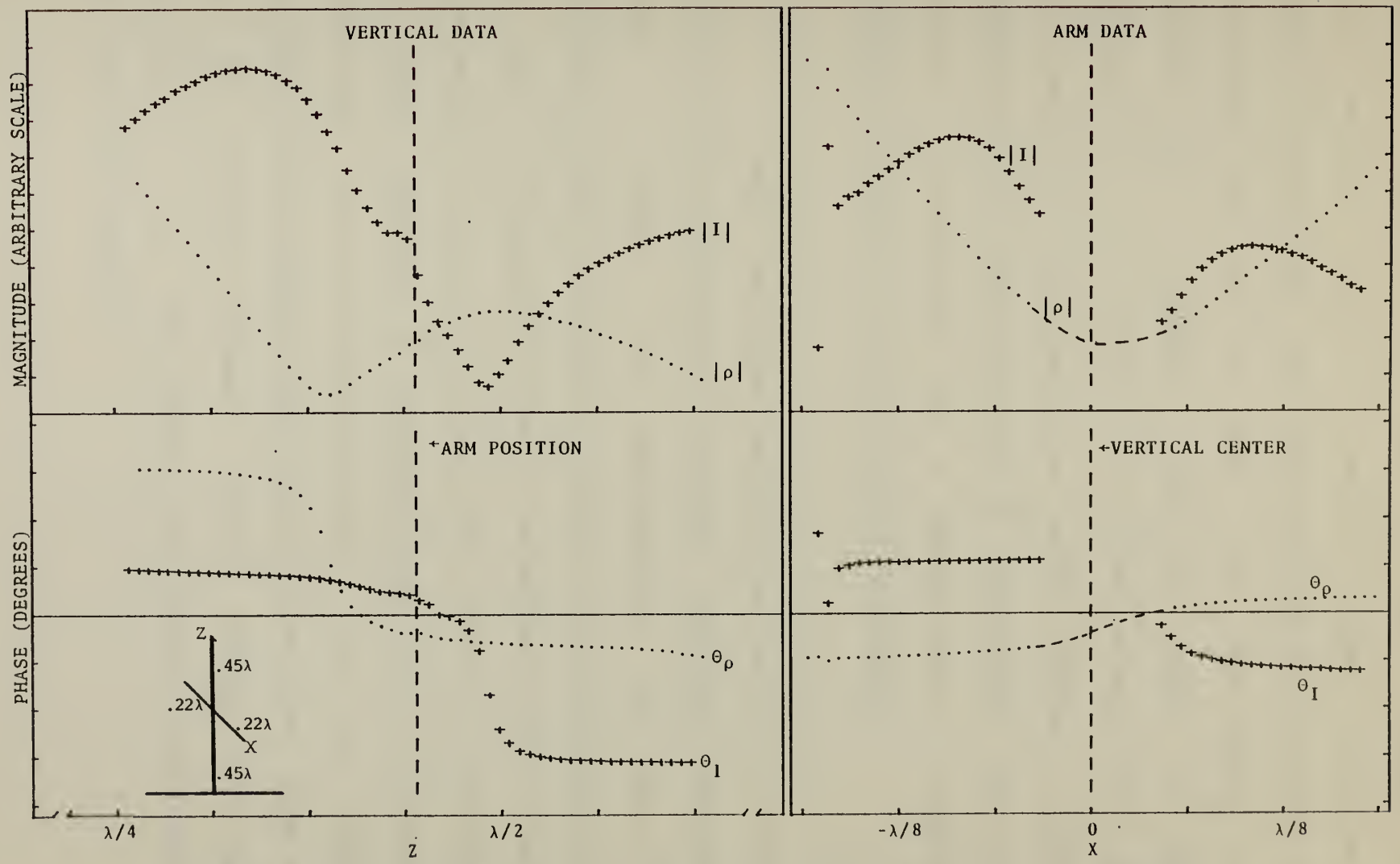

Figure 27. - Measured charge and current density distributions for Case 4 crossed-monopole

Repeated attempts to get smooth data near the upper cross arm end resulted in widely fluctuating readings indicating a measure of instability. The large standing wave pattern and inconsistent data on the upper cross arm signify the presence of a resonant condition unique to this configuration. It is difficult to state categorically why this combination of dimensions should produce a greater response than the other cases but it conceivable that the response is associated with a combination of segments combining to produce a strong resonant structure.

Near the segment extremities the current values do tend toward a minimum as the charge magnitude increases toward a maximum. This configuration, with only 1/4 wavelength cross arm segments, provided the sole opportunity to take data reasonably close to the segment ends, allowing observation of the developing end point boundary conditions. The vector addition of currents fails again in this case (Figure 28). Here the rapid phase shift above the junction combined with an apparent phase shift on the lower cross arm near the junction forecast problems similar to those incurred in Case 3 when sampling the current some distance away from the junction.

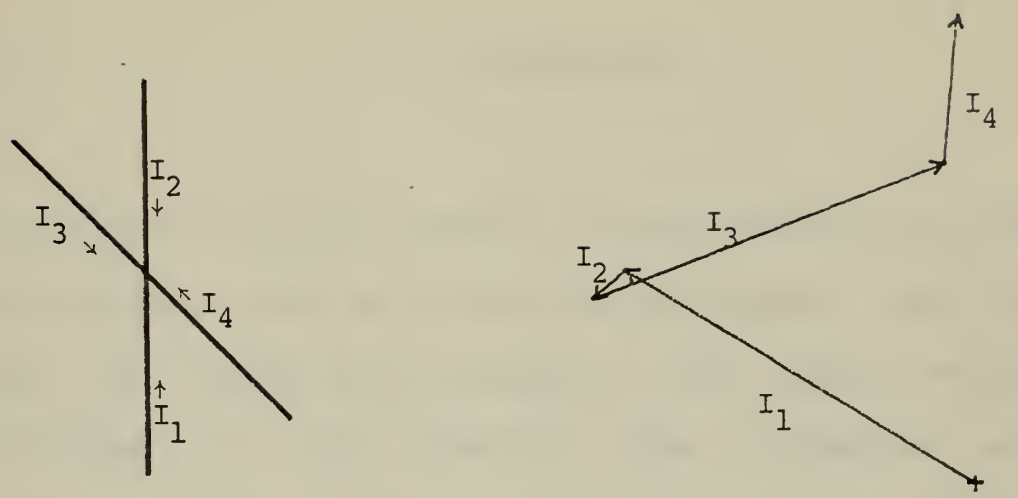

Figure 28. - Application of Kirchoff's Current Law at junction of Case 4 crossed-monopole

IV. CONCLUSIONS

Charge and current density distributions on base fed monopole antennas can be altered significantly with the addition of cross arm segments. The charge density distributions on the monopole are disturbed more significantly when the junction is placed at the position of a current maximum/charge minimum while the charge density distribution variation on the monopole maintains the same general form independent of the position of the junction or length of the cross arms. The oblique intersection of the cross arms results in asymetrical distributions along the arm segments highlighted by the interaction between the lower cross arm and the lower vertical segment, a result of the current magnitude peak being largest just below the junction on the vertical element adjacent to the lower cross arm. Standing wave patterns of varying magnitudes are induced on the antenna segments depending on their electrical length.

The feed point impedance of the base fed crossed-monopole can be varied by changing the angle of

intersection between vertical and cross members. Such a phenomenon could be practically applied to situations where impedance matching is an important consideration. Where inductive coupling is significant between members, it determines the distributions on the cross arms with little regard to the length of the arm. Also, resonant and unstable conditions may occur unexpectedly on some non-orthogonal configurations. The importance of considering inductive coupling when analyzing the possible resonant conditions on non-orthogonal structures has thus been demonstrated.

V. RECOMMENDATIONS

Nonavailibility of the required test apparatus precluded recording far field patterns for the crossed-monopoles as originally intended. Pattern recording ranges exist at Naval Electronics Laboratory Center (NELC), San Diego, California and, subject to their availability, the collection of radiation pattern data would provide information required to assess the possibility of using crossed-monopoles as antennas in special applications where a standard monopole is not suitable.

When dealing with moderately thick antennas it would be advantageous to have a better method of measuring charge and current density distributions. The method used in this thesis would suffice if rotational symmetry can be assumed at all locations on the antennas. This is not the case for the antennas studied at locations near the junction where accurate data would be of most value. The use of infrared imagery to record I^2R heating holds the promise of solving this problem and its application to similar investigations should be pursued.

APPENDIX A

DATA PROCESSING PROGRAMS

This appendix contains a listing of the computer programs used for processing and displaying the data acquired during the course of this thesis research. The programs were written for the Hewlett Packard 9821A Calculator, however the algorithms could easily be translated into another language. The major programming task was performed by LCDR Elmer J. McDowell in connection with thesis research at Naval Postgraduate School, Monterey, CA. The programs listed are modifications of McDowell's work and are included here to provide assistance in any similar investigations.

1. Program to Input Charge and Current Data to Memory

```
 0:  PRT "INSTRUCTIONS"; SPC 1; ▪BEL; ▪BEL
 1:  PRT "WHEN BELL SOUNDS ";" READ TAPE PRINT-"
 2:  PRT "OUT FOR INFORMA-","TION REQUIRED","TO
     ANSWER","INQUIRES" SPC 3
 3:  PRT "PROGRAM TO","INPUT BOTH","CHARGE AND"," CURRENT
     DATA","TO MEMCRY "
 4:  0 → A; SPC 2
 5:  0 → RA; JMP (A + 1 → A) > 499
 6:  0 → A; FXD 3; SPC 2
 7:  PRT "1 → ARM DATA", "0 → VERTICAL DATA"; ▪BEL; ▪BEL;
     SPC 2
 8:  ENT "ARM OR VERTICAL?",R490
 9:  ENT "FREQ. (MHZ) = ?",R480
10:  PRT "ALL DIMENSIONS","IN CENTIMETERS"; ▪BEL; ▪BEL SPC 2
11:  ENT "ANT. HEIGHT = ?",R481
12:  ENT "JUNCTION HT. ?",R482,"RIGHT ARM LGTH ?",R483
13:  ENT "LEFT ARM LGTH ?",R484
14:  PRT "PROBE 0 POS."; ▪BEL; ▪BEL;
15:  IF R490 ≤ 0.5; PRT "MEASURED UP FROM", "GROUND PLANE";
     SPC 2
16:  IF R490 > 0.5; PRT "MEASURE FROM THE", "CENTER OF THE",
     "JUNCTION"
17:  SPC 2
18:  ENT "I PROBE 0 POS. ?",R485
19:  ENT "Q PROBE 0 POS. ?",R486,"ANT. RADIUS = ?",R487
20:  PRT "DATA RECORD"; SPC 2
21:  IF R490 = 0; PRT "VERTICAL MEMBER"; SPC 2; GTO +2
22:  PRT "CROSS ARM";SPC 2
23:  PRT "ANT. HEIGHT =",R481,"ANT. RADIUS =",R487,"LOWER
     CROSS ARM"
24:  PRT "LENGTH =",R483,"UPPER CROSS ARM","LENGTH =",R484
25:  PRT "JUNCTION HT. =",R482;SPC 1
```

```
26:  PRT "FREQUENCY",R480,"MEGAHERTZ"; SPC 2
27:  PRT "0 → CHARGE", "1 → CURRENT"; SPC 2; ▪BEL; ▪BEL;
     ENT "CHG OR CUR DATA?", X; 0 → A
28:  JMP 13X+1
29:  SPC 3; PRT "DATA READOUT IN","FOLLOWING FORMAT"; SPC 1
30:  PRT"REL POSITION", "       MAGNITUDE",
     "           PHASE" ; SPC 2
31:  PRT "CHARGE DATA"; SPC 1
32:  ENT "REL. Q POSITION?",RA;IF FLG 13; A → R488; CFG 13;
     GTO +8
33:  IF A = 0; GTO +2
34:  IF ABS (RA-R(A-1))>1.2;  IF FLG 3 = 0; ▪BEL; GTO -2
35:  ENT "Q MAGNITUDE ?",R(80+A);
     IF ABS (R(80+A)-R(79+A)) > 1; IF A > 0; IF FLG 3 = 0;
     ▪BEL; GTO +0
36:  ENT "QPHASE ?",R(160+A);  IF ABS(R(160 + A)) > 150;
     GTO +2
37:  IF ABS (R(160 + A) - R(159 + A)) > 35; IF A > 0;
     IF FLG 3 = 0; ▪BEL; GTO -1
38:  PRT RA, R(80 + A), R(160 + A); SPC 1; A + 1 → A;
     IF A ≤ 79; GTO -6
39:  PRT "CHARGE STORAGE","REGISTERS FILLED"; A → R488;SPC 2
40:  PRT "0 → NO", "1 → YES"; SPC 2; ▪BEL; ▪BEL;
     ENT "INPUT COMPLETE ?", C; IF C = 0; GTO -13
41:  GTO +11
42:  PRT"REL POSITION", "       MAGNITUDE",
     "           PHASE" ; SPC 2
43:  PRT "CURRENT DATA"; SPC 1
44:  ENT "REL. I POSITION?",  R(240 + A); IF FLG 13;
     A → R489; CFG 13; GTO -4
45:  IF ABS (R(240 + A) - R(239 + A)) > 1.2;  IF A > 0;
     IF FLG 3 = 0; ▪BEL; GTO -1
46:  ENT "I MAG", R(320 + A);
     IF ABS (R(320 + A)) > 1; IF A > 0;
     IF FLG 3 = 0; GTO +0
```

```
47:  ENT "I PHASE ?",R(400  + A); IF ABS(R(400 + A)) > 150;
     GTO +2
48:  IF ABS (R(400 + A) - R(399 + A)) > 35; IF A > 0;
     IF FLG 3 = 0; ▪BEL; GTO -1
49:  PRT R(240 + A), R(320 + A), R(400 + A; SPC 1
50:  A + 1 → A; IF A ≤ 79; GTO -6
51:  PRT "CURR. STORAGE","REGISTERS FILLED";A → R489; SPC 2;
     GTO -11
52:  ENT "TO WHICH TAPE ?",Y; SPC 15
53:  ENT "TO WHAT FILE ?",X;PRT "DATA STORED ON",
     "TAPE NO.",Y,"IN FILE NO.",X
54:  SPC 15; ▪RCF X, R0, R499
55:  ENT "COLUMN PRINTOUT?", X IF ≤ .5; GTO +14
56:  0 → Y → B
57:  0 → A; IF Y > 2.5; 1 → B
58:  IF Y = 0; PRT "CHARGE DATA"; GTO +6
59:  IF Y = 1; GTO +6
60:  IF Y = 2; GTO +6
61:  IF Y = 3; SPC 8; PRT "CURRENT DATA"; GTO +3
62:  IF Y = 4; GTO +3
63:  IF Y = 5; GTO +3
64:  SPC 2; PRT "              POS"; SPC 1; GTO +3
65:  SPC 5; PRT "              MAG"; SPC 1; GTO +2
66:  SPC 5; PRT"          PHASE"; SPC1
67:  PRT R(80Y + A); PRT "----------------";
     JMP (A + 1 → A) = R(488 + B)
68:  Y + 1 → Y; IF ≤ 5; GTO -11
69:  SPC 15; END
```

2. Program to Plot Charge and Current Data

```
 0:  FXD 3; SPC 1
 1:  TBL 4
 2:  ENT "TAPE NO. ?", X, "FILE NO. ?", Y; LDF Y; .4 → R494;
     .007 → R495
 3:  PRT "TAPE NO.", X, "DATA FILE NO.", Y; SPC 1;
     3E4/R480 → R491; JMP R490 + 1
 4:  PRT "VERT, DATA PLOT"; GTO +2
 5:  PRT "ARM DATA PLOT"
 6:  SPC 1; PRT "FREQUENCY (MHZ) =",R480,=LAMBDA (CM.) =",
     R491; SPC 1
 7:  PRT "ANT. HEIGHT =",R481/R491, "       LAMBDA"; SPC 1
 8:  PRT "ANT. RADIUS =",R487/R491, "       LAMBDA"; SPC 1
 9:  PRT "RIGHT ARM LNGTH=", R483/R491, "        LAMBDA";
     SPC 1
10:  PRT "LEFT ARM LENGTH=", R484/R491, "           LAMBDA";
     SPC 1
11:  PRT "JUNCTION HGT =",R482/R491,        LAMBDA"; SPC 1
12:  ENT "SUPRESS AXIS?", X
13:  SCL 30,165.8,0,2.2; IF X = 1; GTO +33
14:  ENT "PLOT LIMITS SET?",Z
15:  PLT 30,0; PLT 32,0; LTR 32,0,211; PLT ",,"; PLT 33.6,0;
     PLT 101,0; LTR 101,0,211; PLT ",,"
16:  PLT 102.4,0;  PLT 105,0; PEN; PLT 105.8,0; PLT 165.8,0;
     PLT 165.8,2.2;  PLT 105.8,2.2; PEN
17:  PLT 105,2.2; PLT 30,2.2; PLT 30,0; PEN; PLT 30,1.1;
     PLT 105,1.1; PEN
18:  PLT 105.8,1.1; PLT 165.8,1.1; PEN; PLT 105.8,0
19:  PLT 105.8,2.2; PEN; PLT 105,2.2; PLT 105,0; PEN
20:  PLT 30,.55; PLT 105,.55; PEN; PLT 105.8,.55
21:  PLT 165.8,.55; PEN
22:  .1 → A → B; 1 → C → X → Y; 30 → Z
```

```
23:  PLT 165.3,1.1 + A; PLT 165.8,1.1 + A; PEN;
     JMP (A + .1 → A) = 1.1
24:  PLT 30,1.1 + B; PLT 30.5,1.1 + B; PEN;
     JMP (B + .1 → B) > 1
25:  PLT Z,.55 + .130263CY; PLT Z + .5,.55 + .130263CY; PEN
26:  C + 1 → C; IF 5 > C; GTO -1
27:  IF Y > 0; -1 → Y; 1 → C; GTO -2
28:  IF 50 > Z; 165.3 → Z; 1 → Y → C; GTO -3
29:  1 → A → C; 1.1 → B
30:  PLT CAR491/16 + 135.8,B + .015;
     PLT CAR491/16 + 135.8,B; PEN
31:  A + 1 → A; IF 30 > AR491/16; GTO -1
32:  IF C > 0; -1 → C; 0 → A; GTO -2
33:  IF B > 0; 0 → B; 1 → C → A; GTO -3
34:  1 → A; 1.1 → B
35:  A + 1 → A → Y; JMP AR491/16 > 35
36:  PLT AR491/16, B + .015; PLT AR491/16,B; PEN; A + 1 → A;
     JMP AR491/16 > 105
37:  IF B > 0; 0 → B; Y → A; GTO -1
38:  2.1 → Y; R482 → X; GTO +2
39:  135.8 → X; 2.1 → Y
40:  PLT X,Y; PLT X,Y - .03; PEN; JMP (Y - .06 → Y) ≤ 1.15
41:  1.05 → Y
42:  PLT X,Y; PLT X,Y - .03; PEN; JMP (Y - .06 → Y) ≤ .05
43:  IF X ≤ 100; GTO -4
44:  LTR 144,2.15,111
45:  LTR 157.5 - R494,2.1 - R495,111; PEN
46:  0 → A → B → C
47:  R485 - R(240 + A) → R(240 + A); JMP (A + 1 → A) = R489
48:  ENT "IMAG SCL FACTOR?", Z; PRT "IMAG SCL FACTOR=", Z;
     SPC 1; IF Z = 1; GTO +2
49:  ZR(320 + C) → R(320 + C); JMP (C + 1 → C) = R489
50:  IF R(320 + B) > R493; R(320 + B) → R493
51:  B + 1 → B; IF B ≤ R489 - 1; GTO -1
52:  PRT "MAXIMUM CURRENT", "MAGNITUDE =", R493; SPC 1
53:  ENT "IMAG GRAPHLIMIT?", Z; IR 1.1Z > R493; Z → R493
```

```
54:  PRT "REF. CURRENT", "MAX MAGNITUDE =", R493; SPC 1
55:  0 → A → B → C → X → Y; 135.8 * R490 → Z
56:  LTR R(240 + A) - R494 + Z,1.1 + R(320 + A) / R493 -
     R495,111; PLT "+"; JMP (A + 1 → A) = R489
57:  R486 - RB → RB; JMP (B + 1 → B) = R488
58:  ENT "QMAG SCL FACTOR?, Z; PRT "QMAG SCL FACTOR=", Z;
     SPC 1; IF Z = 1; GTO +2
59:  ZR(80 + C) → R(80 + C); JMP (C + 1 → C) = R489
60:  IF R(80 + X) > R492; R(80 + X) → R492
61:  X + 1 → X; IF X ≤ R489 - 1; GTO -1
62:  PRT "MAXIMUM CHARGE", " MAGNITUDE =", R492; SPC 1
63:  ENT "QMAG GRAPHLIMIT?", Z; IF 1.1Z > R492; Z → R492
64:  PRT "REF. CHARGE", "MAX MAGNITUDE =", R492; SPC 1
65:  135.8 * R490 → X
66:  PLT X + RY, 1.1 + R(80 + Y) / R492; PEN;
     JMP (Y + 1 → Y) = R488
67:  ENT "SLIDE PHASE ? DEG", Z; 0 → A → B; 400 → C
68:  ENT "I PHASE CORR = ?", X, "Q PHASE CORR = ?", Y
69:  PRT "PHASE SLID BY", Z; PRT "      DEGREES"; SPC1
70:  PRT "CHARGE PHASE", "CORRECTED BY", Y; SPC 1
71:  PRT "CURRENT PHASE", "CORRECTED BY", X; SPC 1
72:  R(C + A) + Z + X → R(C + A); IF R490 = 1; IF C > 300;
     IF R(240 + A) > 0; R(C + A) + 180 → R(C + A)
73:  IF R(C + A) > -180; GTO +2
74:  R(C + A) + 360 → R(C + A); GTO -1
75:  IF R(C + A) ≤ 180; GTO +2
76:  R (C + A) - 360 → R(C + A); GTO -1
77:  A + 1 → A; IF A ≤  R(489 - B) - 1; GTO -5
78:  IF C > 300; 160 → C; 0 → A; 1 → B; Y → X; GTO -6
79:  0 → A → B; 135.8 * R490 → X
80:  LTR R(240 + A) - R494 + X, .55 + R(400 + A) / 380 -
     R495,111; PLT "+"; JMP (A + 1 → A) = R489
81:  PEN; PLT X + RB, .55 + R(160 + B) / 380;
     JMP (B + 1 → B) = R488
82:  PEN; SPC 13; END
```

3. Memory Allocation

REGISTER	CONTENT
0-79	Charge Position
80-159	Charge Magnitude
160-239	Charge Phase
240-319	Current Position
320-399	Current Magnitude
400-479	Current Phase
480	Frequency (Megahertz)
481	Antenna Height (cm)
483	Right Arm Length
482	Junction Height
484	Left Arm Length
485	Current Probe Zero Position
486	Charge Probe Zero Position
487	Antenna Radius
488	Number of Charge Data Points
489	Number of Current Data Points
490	Vertical Data (0); Arm Data (1)
491	Wavelength
492	Maximum Charge Magnitude
493	Maximum Current Magnitude
494	Vertical Correction for "+" character
495	Horizontal Correction for "+" Character
496	(Empty)
497	(Empty)
498	(Empty)
499	(Empty)

APPENDIX B

NUMERICAL DATA

This appendix contains the numerical data for the four configurations investigated. Position is given in centimeters above the ground plane for vertical data and centimeters to the right (positive) or left (negative) of the junction for arm data. Magnitude values indicate relative signal strength and phase measurements indicate relative phase with respect to the reference, a sample of the antenna exitation signal.

CASE 1 VERTICAL CHARGE DATA

POSITION (cm)	MAGNITUDE (rel.)	PHASE (deg)	POSITION (cm)	MAGNITUDE (rel.)	PHASE (deg)
97.00	2.22	-46.4	69.00	1.21	35.5
96.00	2.24	-45.5	68.00	1.21	41.3
95.00	2.25	-44.2	67.00	1.27	55.5
94.00	2.25	-43.0	66.00	1.31	57.5
93.00	2.24	-41.7	65.00	1.37	61.3
92.00	2.23	-40.5	64.00	1.44	65.3
91.00	2.20	-39.1	63.00	1.52	69.6
90.00	2.17	-37.6	62.00	1.62	74.1
89.00	2.14	-36.1	61.00	1.73	78.5
88.00	2.10	-34.6	60.00	1.85	82.9
87.00	2.05	-33.0	59.00	2.02	87.5
86.00	2.01	-31.2	58.00	2.15	91.4
85.00	1.94	-29.5	57.00	2.30	94.9
84.00	1.88	-27.1	56.00	2.49	98.0
83.00	1.81	-25.0	55.00	2.66	100.2
82.00	1.75	-22.6	54.00	2.85	103.0
81.00	1.68	-20.1	53.00	3.03	105.4
80.00	1.61	-17.1	52.00	3.20	107.5
79.00	1.54	-14.2	51.00	3.36	109.5
78.00	1.47	-11.0	50.00	3.53	111.5
77.00	1.42	-7.4	49.00	3.68	113.3
76.00	1.36	-3.6	48.00	3.82	115.0
75.00	1.32	.4	47.00	3.95	116.5
74.00	1.28	4.0	46.00	4.08	118.0
73.00	1.25	8.0	45.00	4.18	119.3
72.00	1.20	14.8	44.00	4.29	121.0
71.00	1.18	20.0	43.00	4.37	122.5
70.00	1.18	26.6	42.00	4.45	123.9
			41.00	4.51	125.3

CASE 1 VERTICAL CURRENT DATA

POSITION (cm)	MAGNITUDE (rel.)	PHASE (deg)	POSITION (cm)	MAGNITUDE (rel.)	PHASE (deg)
95.20	.53	-81.8	67.20	1.65	-5.6
94.20	.55	-72.0	66.20	1.56	-3.1
93.20	.58	-62.6	65.20	1.44	-3.1
92.20	.62	-54.4	64.20	1.57	-1.3
91.20	.68	-48.0	63.20	1.71	.3
90.20	.74	-41.6	62.20	1.89	1.7
89.20	.79	-36.6	61.20	2.08	3.0
88.20	.86	-32.5	60.20	2.26	4.0
87.20	.92	-28.9	59.20	2.40	4.9
86.20	.99	-25.8	58.20	2.53	5.9
85.20	1.05	-23.3	57.20	2.60	6.9
84.20	1.11	-21.2	56.20	2.64	7.9
83.20	1.15	-19.2	55.20	2.64	9.0
82.20	1.20	-18.1	54.20	2.62	10.4
81.20	1.23	-16.6	53.20	2.57	11.8
80.20	1.26	-15.7	52.20	2.52	13.2
79.20	1.27	-15.1	51.20	2.43	14.8
78.20	1.27	-14.8	50.20	2.34	16.6
77.20	1.26	-14.6	49.20	2.23	18.7
76.20	1.23	-14.7	48.20	2.11	21.2
75.20	1.20	-15.0	47.20	1.98	23.8
74.20	1.17	-15.0	46.20	1.86	26.8
73.20	1.15	-14.8	45.20	1.72	30.6
72.10	1.11	-14.3	44.20	1.59	34.5
71.20	1.08	-13.6	43.20	1.46	39.3
70.20	1.32	-10.6	42.20	1.33	45.5
69.20	1.47	-9.1	41.20	1.21	53.0
68.20	1.59	-7.1	40.20	1.12	61.9

CASE 1 CROSS ARM CHARGE DATA

POSITION (cm)	MAGNITUDE (rel.)	PHASE (deg)	POSITION (cm)	MAGNITUDE (rel.)	PHASE (deg)
28.50	3.98	150.5	-6.2	1.77	98.9
27.50	3.83	150.4	-7.20	1.90	97.7
26.50	3.65	150.1	-8.20	2.03	96.8
25.50	3.50	149.8	-9.20	2.19	95.9
24.50	3.36	149.6	-10.20	2.35	95.0
23.50	3.23	149.4	-11.20	2.52	94.4
22.50	3.31	149.0	-12.20	2.70	93.6
21.50	2.97	148.6	-13.20	2.89	93.1
20.50	2.86	148.5	-14.20	3.07	92.5
19.50	2.73	148.2	-15.20	3.25	92.1
18.50	2.60	148.0	-16.20	3.44	91.6
17.50	2.47	147.6	-17.20	3.62	91.2
16.50	2.35	147.1	-18.20	3.81	90.7
15.50	2.22	146.7	-19.20	4.00	90.3
14.50	2.10	146.2	-20.20	4.20	89.8
13.50	1.97	145.5	-21.20	4.40	89.4
12.50	1.84	144.8	-22.20	4.59	89.1
11.50	1.71	143.7	-23.20	4.79	88.8
10.50	1.59	142.6	-24.20	5.00	88.5
9.40	1.46	141.0	-25.20	5.27	87.9
8.40	1.37	139.5	-26.20	5.60	85.6
			-27.20	5.30	90.1
			-28.20	5.75	89.1

CASE 1 CROSS ARM CURRENT DATA

POSITION (cm)	MAGNITUDE (rel.)	PHASE (deg)	POSITION (cm)	MAGNITUDE (rel.)	PHASE (deg)
27.00	1.33	-110.4	-5.20	2.16	-174.5
26.00	1.37	-110.2	-6.20	2.31	-174.4
25.00	1.45	-110.0	-7.20	2.46	-174.5
24.00	1.51	-109.4	-8.20	2.62	-174.6
23.00	1.57	-108.5	-9.20	2.77	-174.9
22.00	1.64	-108.2	-10.20	2.88	-175.0
21.00	1.69	-108.1	-11.20	2.95	-175.2
20.00	1.72	-106.9	-12.20	2.99	-175.2
19.00	1.76	-106.7	-13.20	3.00	-175.3
18.00	1.79	-106.1	-14.20	3.00	-175.6
17.00	1.80	-105.2	-15.20	2.97	-175.7
16.00	1.81	-104.3	-16.20	2.93	-175.9
15.00	1.80	-103.3	-17.20	2.88	-176.0
14.00	1.77	-102.0	-18.20	2.81	-176.1
13.00	1.72	-100.5	-19.20	2.73	-176.2
12.00	1.66	-98.5	-20.20	2.65	-176.5
11.00	1.56	-95.9	-21.20	2.57	-176.9
10.00	1.43	-92.0	-22.20	2.49	-177.5
9.00	1.27	-85.2	-23.20	2.39	-178.3
8.00	1.10	-75.2	-24.20	2.35	179.5
7.00	.98	-62.5	-25.20	2.25	177.0
			-26.20	2.90	141.0
			-27.20	.70	-146.5

CASE 2 VERTICAL CHARGE DATA

POSITION (cm)	MAGNITUDE (rel.)	PHASE (deg)	POSITION (cm)	MAGNITUDE (rel.)	PHASE (deg)
97.50	1.95	-86.0	68.50	.62	8.1
96.50	1.96	-85.2	67.50	.62	25.9
95.50	1.97	-83.9	66.50	.69	53.5
94.50	1.97	-82.9	65.50	.74	58.8
93.40	1.96	-81.7	64.50	.82	66.4
92.50	1.95	-80.7	63.50	.93	73.9
91.50	1.93	-79.3	62.50	1.08	81.7
90.50	1.90	-78.0	61.50	1.27	89.4
89.50	1.87	-76.9	60.50	1.47	95.4
88.50	1.84	-75.2	59.50	1.65	99.1
87.50	1.79	-73.7	58.50	1.74	100.1
86.50	1.74	-72.3	57.40	1.93	102.6
85.50	1.69	-71.4	56.50	2.11	105.6
84.50	1.62	-69.6	55.50	2.35	108.4
83.50	1.57	-67.2	54.50	2.68	111.9
82.50	1.50	-65.0	53.50	2.91	113.8
81.50	1.44	-62.9	52.50	3.15	115.8
80.50	1.37	-60.5	51.50	3.38	117.4
79.50	1.30	-57.9	50.50	3.58	118.5
78.50	1.23	-54.9	49.50	3.80	119.8
77.50	1.15	-51.6	48.50	3.97	121.1
76.50	1.08	-47.9	47.50	4.14	122.2
75.50	1.02	-44.0	46.50	4.29	123.0
74.50	.95	-39.6	45.50	4.44	124.0
73.50	.90	-34.9	44.50	4.58	124.9
72.50	.84	-29.9	43.50	4.71	125.8
71.50	.75	-22.8	42.50	4.82	126.6
70.50	.69	-15.0	41.50	4.94	127.5
69.50	.65	-5.5	40.50	5.00	128.0

CASE 2 VERTICAL CURRENT DATA

POSITION (cm)	MAGNITUDE (rel.)	PHASE (deg)	POSITION (cm)	MAGNITUDE (rel.)	PHASE (deg)
96.70	.58	-98.6	67.70	1.67	35.1
95.70	.55	-91.3	66.70	1.62	37.3
94.60	.54	-82.1	65.70	1.58	38.9
93.70	.53	-74.4	64.70	1.60	41.5
92.70	.53	-65.9	63.60	1.78	44.0
91.70	.55	-57.7	62.70	1.95	45.8
90.70	.57	-50.2	61.70	2.15	47.7
89.70	.60	-43.1	60.70	2.36	49.1
88.70	.63	-36.8	59.70	2.54	50.6
87.70	.67	-31.6	58.70	2.69	51.8
86.70	.71	-26.5	57.60	2.82	52.5
85.70	.74	-22.3	56.70	2.86	53.5
84.70	.78	-18.7	55.70	2.88	54.3
83.70	.82	-15.1	54.70	2.86	55.1
82.70	.86	-12.0	53.70	2.83	55.9
81.70	.89	-9.0	52.70	2.78	56.9
80.70	.92	-6.3	51.70	2.69	57.9
79.70	.94	-3.7	50.70	2.60	58.9
78.70	.96	-1.2	49.70	2.48	60.1
77.70	.97	1.3	48.70	2.36	61.4
76.70	.98	4.0	47.70	2.23	62.7
75.70	.98	6.6	46.70	2.08	64.4
74.70	.98	9.4	45.70	1.93	66.1
73.70	.98	12.2	44.70	1.76	68.4
72.70	.99	14.8	43.70	1.61	71.2
71.70	.99	17.2	42.70	1.44	74.5
70.70	.98	18.9	41.70	1.28	78.4
69.70	1.28	25.1	40.70	1.10	84.1
68.70	1.46	29.5	39.70	.95	91.2

CASE 2 CROSS ARM CHARGE DATA

POSITION (cm)	MAGNITUDE (rel.)	PHASE (deg)	POSITION (cm)	MAGNITUDE (rel.)	PHASE (deg)
28.75	2.27	-37.1	-7.05	.81	-2.5
28.25	2.22	-36.8	-8.05	.86	-5.4
27.25	2.15	-36.0	-9.05	.92	-8.5
26.25	2.10	-35.3	-10.05	.97	-11.0
25.25	2.03	-34.4	-11.05	1.02	-13.2
24.25	1.96	-33.1	-12.05	1.08	-15.3
23.25	1.88	-31.5	-13.05	1.12	-16.6
22.25	1.79	-31.0	-14.05	1.16	-18.0
21.25	1.72	-28.5	-14.95	1.20	-19.0
20.25	1.64	-25.5	-16.05	1.24	-20.6
19.25	1.55	-24.3	-16.95	1.27	-21.2
18.25	1.46	-21.0	-18.05	1.31	-23.5
17.25	1.38	-18.3	-19.05	1.34	-24.6
16.25	1.30	-15.4	-20.05	1.35	-25.4
15.25	1.22	-11.0	-21.05	1.36	-26.0
14.25	1.14	-6.2	-22.05	1.37	-26.6
13.25	1.06	-2.3	-23.05	1.38	-27.2
12.25	.99	1.9	-24.05	1.37	-27.8
11.25	.92	6.4	-25.05	1.37	-28.0
10.25	.85	10.9	-26.05	1.35	-28.5
9.25	.80	14.8	-27.05	1.34	-30.0
8.25	.75	17.8	-28.05	1.30	-30.2
			-29.05	1.26	-30.5

CASE 2 CROSS ARM CURRENT DATA

POSITION (cm)	MAGNITUDE (rel.)	PHASE (deg)	POSITION (cm)	MAGNITUDE (rel.)	PHASE (deg)
28.40	1.10	40.0	-5.80	.90	32.0
27.40	1.14	41.0	-6.80	.84	32.6
26.40	1.22	42.8	-7.80	.77	33.5
25.40	1.29	44.5	-8.80	.71	34.5
24.30	1.36	46.0	-9.80	.65	35.5
23.40	1.41	47.0	-10.80	.59	36.2
22.40	1.47	48.3	-11.80	.53	36.3
21.40	1.52	49.5	-12.80	.48	35.8
20.30	1.59	50.8	-13.80	.43	34.6
19.40	1.62	51.6	-14.80	.38	32.3
18.40	1.66	52.5	-15.80	.33	28.9
17.40	1.69	53.4	-16.80	.29	23.8
16.40	1.71	54.4	-17.80	.25	16.8
15.40	1.71	55.4	-18.80	.22	6.3
14.40	1.69	56.3	-19.80	.20	-4.7
13.40	1.66	57.4	-20.80	.19	-19.6
12.40	1.59	58.6	-21.80	.19	-35.0
11.40	1.50	60.1	-22.80	.21	-48.5
10.40	1.36	62.0	-23.80	.24	-59.6
9.30	1.15	65.0	-24.80	.28	-68.2
8.40	.97	68.5	-25.80	.31	-74.6
7.40	.72	75.5	-26.80	.36	-79.2
6.40	.49	89.7	-27.80	.40	-83.2
			-28.80	.45	-86.2

CASE 3 VERTICAL CHARGE DATA

POSITION (cm)	MAGNITUDE (rel.)	PHASE (deg)	POSITION (cm)	MAGNITUDE (rel.)	PHASE (deg)
97.95	.81	160.1	68.95	1.72	-158.8
96.95	.85	162.7	67.95	1.79	-154.5
95.95	.90	165.0	66.95	1.81	-154.3
94.95	.95	167.6	65.95	1.85	-153.5
93.95	.99	170.1	64.95	1.90	-151.2
92.95	1.02	172.0	63.95	1.96	-151.2
91.95	1.07	173.9	62.95	2.03	-149.5
90.95	1.11	175.4	61.95	2.10	-147.7
89.85	1.16	177.2	60.95	2.17	-145.9
88.85	1.20	178.8	59.95	2.24	-144.2
87.95	1.23	-179.8	58.95	2.28	-142.9
86.85	1.27	-177.7	57.85	2.34	-141.0
85.95	1.30	-176.9	56.95	2.39	-139.3
84.85	1.32	-175.6	55.95	2.47	-137.3
83.85	1.36	-174.4	54.95	2.58	-135.0
82.95	1.39	-173.2	53.95	2.65	-133.1
81.95	1.42	-172.0	52.95	2.72	-131.4
80.95	1.45	-171.0	51.95	2.80	-129.6
79.95	1.46	-170.0	50.95	2.86	-128.0
78.95	1.48	-168.9	49.95	2.94	-126.4
77.95	1.50	-167.9	48.95	2.99	-124.9
76.95	1.53	-167.0	47.95	3.04	-123.4
75.95	1.55	-166.0	46.95	3.10	-122.9
74.95	1.57	-165.0	45.95	3.15	-120.3
73.95	1.59	-164.3	44.95	3.21	-118.6
72.95	1.60	-163.5	43.95	3.27	-117.2
71.95	1.61	-162.1	42.95	3.34	-115.9
70.95	1.63	-161.2	41.95	3.38	-114.5
69.95	1.66	-160.2	40.95	3.41	-113.4

CASE 3 VERTICAL CURRENT DATA

POSITION (cm)	MAGNITUDE (rel.)	PHASE (deg)	POSITION (cm)	MAGNITUDE (rel.)	PHASE (deg)
96.70	.78	139.0	67.70	.85	-175.0
95.70	.81	139.6	66.70	.83	-173.0
94.70	.82	141.3	65.70	.75	-171.9
93.70	.84	142.3	64.70	.81	-169.2
92.70	.83	143.5	63.70	.89	-166.9
91.70	.82	144.8	62.70	.99	-165.0
90.70	.79	146.2	61.70	1.08	-163.1
89.70	.78	147.1	60.70	1.18	-161.8
88.70	.77	148.3	59.70	1.28	-160.5
87.70	.75	149.7	58.70	1.36	-159.2
86.70	.74	151.4	57.70	1.42	-158.0
85.70	.72	152.9	56.70	1.46	-156.9
84.70	.71	154.3	55.70	1.48	-155.8
83.70	.69	155.6	54.70	1.50	-154.4
82.70	.68	157.1	53.70	1.50	-153.0
81.70	.67	158.5	52.70	1.51	-151.4
80.70	.65	160.1	51.70	1.50	-149.5
79.70	.64	161.6	50.70	1.48	-147.7
78.70	.62	163.0	49.70	1.46	-146.0
77.70	.61	164.2	48.70	1.44	-144.0
76.70	.59	165.4	47.70	1.42	-142.1
75.70	.57	166.5	46.70	1.39	-139.8
74.70	.55	167.6	45.70	1.36	-137.5
73.70	.54	168.9	44.70	1.33	-135.0
72.70	.53	170.5	43.70	1.30	-132.5
71.60	.51	172.4	42.70	1.27	-129.6
70.70	.50	173.6	41.70	1.24	-126.5
69.70	.66	177.9	40.70	1.21	-123.4
68.70	.75	-178.6	39.70	1.18	-120.0

CASE 3 CROSS ARM CHARGE DATA

POSITION (cm)	MAGNITUDE (rel.)	PHASE (deg)	POSITION (cm)	MAGNITUDE (rel.)	PHASE (deg)
29.40	1.11	160.9	-7.10	1.75	-162.5
28.40	1.15	164.0	-8.10	1.74	-163.3
27.40	1.18	167.0	-9.10	1.73	-164.1
26.40	1.22	170.1	-10.10	1.72	-164.9
25.40	1.26	173.2	-11.00	1.70	-165.5
24.40	1.30	176.0	-12.10	1.69	-166.4
23.40	1.33	178.4	-13.10	1.66	-167.1
22.40	1.38	-178.9	-14.10	1.64	-168.0
21.40	1.42	-176.5	-15.10	1.60	-168.8
20.40	1.45	-174.4	-16.10	1.57	-169.7
19.40	1.49	-172.7	-17.10	1.52	-170.6
18.40	1.53	-170.1	-18.10	1.48	-171.6
17.30	1.56	-168.0	-19.10	1.44	-172.5
16.40	1.59	-166.4	-20.10	1.39	-173.5
15.40	1.62	-164.6	-21.10	1.34	-174.4
14.40	1.65	-163.1	-22.10	1.29	-175.5
13.40	1.68	-161.8	-23.10	1.23	-176.6
12.40	1.70	-160.5	-24.10	1.18	-177.8
11.40	1.71	-159.5	-25.10	1.12	-179.1
10.40	1.72	-158.5	-26.10	1.06	179.1
9.40	1.73	-158.0	-27.10	1.00	177.5
8.40	1.74	-157.6	-28.10	.95	175.8
			-29.10	.88	173.7

CASE 3 CROSS ARM CURRENT DATA

POSITION (cm)	MAGNITUDE (rel.)	PHASE (deg)	POSITION (cm)	MAGNITUDE (rel.)	PHASE (deg)
27.90	1.46	164.5	-7.40	.61	166.2
26.90	1.45	164.5	-8.40	.61	162.7
25.90	1.44	165.5	-9.40	.62	159.2
24.90	1.43	166.6	-10.40	.63	156.0
23.80	1.42	167.5	-11.40	.64	153.0
22.90	1.41	168.4	-12.40	.66	150.1
21.90	1.39	169.5	-13.40	.68	147.5
20.90	1.37	171.7	-14.40	.70	145.5
19.90	1.35	172.0	-15.40	.73	143.5
18.90	1.32	173.4	-16.40	.75	141.6
17.80	1.29	174.9	-17.40	.77	139.8
16.90	1.26	175.6	-18.40	.80	138.0
15.90	1.21	177.0	-19.40	.83	136.2
14.90	1.17	178.0	-20.40	.86	134.8
13.90	1.12	179.2	-21.40	.88	133.9
12.90	1.06	-179.6	-22.40	.91	132.6
11.90	1.00	-178.2	-23.40	.94	131.6
10.80	.92	-177.5	-24.40	.96	130.8
9.90	.83	-176.6	-25.4	.98	130.0
8.90	.71	-176.4	-26.40	1.00	129.0
7.90	.57	-176.1	-27.40	1.02	128.5
6.90	.42	-176.3	-28.40	1.03	128.1
5.90	.28	-177.2	-29.40	1.05	127.6

CASE 4 VERTICAL CHARGE DATA

POSITION (cm)	MAGNITUDE (rel.)	PHASE (deg)	POSITION (cm)	MAGNITUDE (rel.)	PHASE (deg)
96.95	.54	90.0	68.95	1.19	116.2
95.95	.62	92.3	67.95	1.12	116.7
94.95	.71	93.1	66.95	.97	116.1
93.95	.79	95.6	65.95	.89	119.5
92.95	.87	96.9	64.95	.79	123.5
91.95	.94	97.8	63.95	.69	128.1
90.95	1.02	98.8	62.95	.58	134.9
89.95	1.09	99.5	61.95	.47	144.2
88.95	1.16	99.8	60.95	.36	160.1
87.95	1.22	100.4	59.95	.29	-173.8
86.95	1.28	100.9	58.95	.31	-138.6
85.95	1.35	101.4	57.95	.42	-114.1
84.95	1.41	101.9	56.95	.57	-100.6
83.95	1.46	102.4	55.95	.76	-92.8
82.95	1.50	102.8	54.95	.95	-87.6
81.95	1.55	103.2	53.95	1.15	-84.0
80.95	1.59	103.6	52.95	1.36	-81.7
79.95	1.62	104.1	51.95	1.57	-80.0
78.95	1.64	104.5	50.95	1.78	-78.5
77.95	1.66	105.0	49.95	1.99	-77.5
76.95	1.66	105.6	48.95	2.20	-76.6
75.95	1.65	106.2	47.95	2.41	-76.8
74.95	1.63	107.0	46.95	2.60	-75.4
73.95	1.60	107.8	45.95	2.81	-74.9
72.95	1.55	108.8	44.95	3.01	-74.5
71.95	1.48	109.5	43.95	3.19	-74.1
70.95	1.42	110.8	42.95	3.39	-73.9
69.65	1.34	112.5	41.95	3.57	-73.6
			40.95	3.77	-73.4

CASE 4 VERTICAL CURRENT DATA

POSITION (cm)	MAGNITUDE (rel.)	PHASE (deg)	POSITION (cm)	MAGNITUDE (rel.)	PHASE (deg)
95.75	1.98	-24.3	67.75	1.90	150.4
94.75	1.96	-24.2	66.75	1.97	152.2
93.75	1.93	-24.0	65.75	1.97	152.9
92.75	1.90	-23.9	64.75	2.08	153.9
91.75	1.86	-23.8	63.75	2.24	156.6
90.75	1.83	-23.6	62.75	2.43	159.4
89.75	1.79	-23.5	61.75	2.65	162.1
88.75	1.74	-23.3	60.75	2.89	164.4
87.75	1.69	-23.1	59.75	3.07	166.2
86.75	1.63	-22.7	58.75	3.26	167.7
85.75	1.56	-22.3	57.75	3.42	168.8
84.75	1.49	-22.0	56.75	3.55	169.8
83.75	1.40	-21.4	55.75	3.62	170.6
82.75	1.31	-20.5	54.75	3.69	171.2
81.75	1.20	-19.4	53.75	3.73	171.8
80.75	1.08	-17.9	52.75	3.75	172.1
79.75	.94	-15.6	51.75	3.76	172.6
78.75	.77	-12.0	50.75	3.75	173.0
77.65	.57	-3.9	49.75	3.74	173.4
76.75	.42	10.5	48.75	3.71	173.7
75.75	.28	45.9	47.75	3.67	174.1
74.75	.33	92.0	46.75	3.62	174.4
73.75	.50	113.3	45.75	3.57	174.8
72.75	.68	123.0	44.75	3.52	175.3
71.75	.85	127.5	43.65	3.44	175.6
70.75	.99	129.8	42.75	3.38	176.0
69.75	1.21	140.8	41.75	3.30	176.5
68.75	1.50	144.9	40.75	3.21	177.0
			39.75	3.12	177.6

CASE 4 CROSS ARM CHARGE DATA

POSITION (cm)	MAGNITUDE (rel.)	PHASE (deg)	POSITION (cm)	MAGNITUDE (rel.)	PHASE (deg)
28.50	3.98	150.5	-6.20	1.77	98.9
27.50	3.83	150.4	-7.20	1.90	97.7
26.50	3.65	150.1	-8.20	2.03	96.8
25.50	3.50	149.8	-9.20	2.19	95.9
24.50	3.36	149.6	-10.20	2.35	95.0
23.50	3.23	149.4	-11.20	2.52	94.4
22.50	3.10	149.0	-12.20	2.70	93.6
21.50	2.97	148.6	-13.20	2.89	93.1
20.50	2.86	148.5	-14.20	3.07	92.5
19.50	2.73	148.2	-15.20	3.25	92.1
18.50	2.60	148.0	-16.20	3.44	91.6
17.50	2.47	147.6	-17.20	3.62	91.2
16.50	2.35	147.1	-18.20	3.81	90.7
15.50	2.22	146.7	-19.20	4.00	90.3
14.50	2.10	146.2	-20.20	4.20	89.8
13.50	1.97	145.5	-21.20	4.40	89.4
12.50	1.84	144.8	-22.20	4.59	89.1
11.50	1.71	143.7	-23.20	4.79	88.8
10.50	1.59	142.6	-24.20	5.00	88.5
9.40	1.46	141.0	-25.20	5.27	87.9
8.40	1.37	139.5	-26.20	5.60	85.6
			-27.20	5.30	90.1
			-28.20	5.75	89.1

CASE 4 CROSS ARM CURRENT DATA

POSITION (cm)	MAGNITUDE (rel.)	PHASE (deg)	POSITION (cm)	MAGNITUDE (rel.)	PHASE (deg)
27.00	1.33	-110.4	-5.20	2.16	-174.5
26.00	1.37	-110.2	-6.20	2.31	-174.4
25.00	1.45	-110.0	-7.20	2.46	-174.6
24.00	1.51	-109.4	-8.20	2.62	-174.6
23.00	1.57	-108.6	-9.20	2.77	-174.9
22.00	1.64	-108.2	-10.20	2.88	-175.0
21.00	1.69	-108.1	-11.20	2.95	-175.2
20.00	1.72	-106.9	-12.20	2.99	-175.2
19.00	1.76	-106.7	-13.20	3.00	-175.3
18.00	1.79	-106.1	-14.20	3.00	-175.6
17.00	1.80	-105.2	-15.20	2.97	-175.7
16.00	1.81	-104.3	-16.20	2.93	-175.9
15.00	1.80	-103.3	-17.20	2.88	-176.0
14.00	1.77	-102.0	-18.20	2.81	-176.1
13.00	1.72	-100.5	-19.20	2.73	-176.2
12.00	1.66	-98.5	-20.20	2.65	-176.5
11.00	1.56	-95.9	-21.20	2.57	-176.9
10.00	1.43	-92.0	-22.20	2.49	-177.5
9.00	1.27	-85.2	-23.20	2.39	-178.0
8.00	1.10	-75.2	-24.20	2.35	179.5
7.00	.98	-62.5	-25.20	2.25	177.0
			-26.20	2.90	141.0
			-27.20	.70	-146.5

BIBLIOGRAPHY

1. Brown, R. G., Sharpe, R. A., Hughes, W. L., and Post, R. E., Lines, Waves, and Antennas, The Transmission of Electric Energy, The Ronald Press Company, New York, 1973.

2. Burton, R. W., "The Crossed-Dipole Structure of Aircraft in an Electromagnetic Pulse Environment," Proceedings of The Conference on Electromagnetic Noise, Interference and Compatibility Advisory Group for Aerospace Research and Development (AGARD) NATO, p. 30-1 thru 30-15, Paris, France, October 1974.

3. Burton, R. W. and King, R. W. P., "Measured Currents and Charges on Thin Crossed Antennas in a Plane-Wave Field," IEEE Transactions on Antennas and Propagation, v. AP-23, No. 5, p. 657 - 664, September 1975.

4. Cruft Laboratory, Harvard University Report Number 377, Electromagnetic Field Probes, by Haven Whiteside, October 1962.

5. Defense Nuclear Agency Report Number 2772T, EMP Awareness Course Notes,, IIT Research Institute, p. 1, August 1971.

6. King, R. W. P., The Theory of Linear Antennas, Harvard University Press, Cambridge, massachusetts, 1956.

7. Mc Dowell, E. J., Charge and Current Distributions on, and Input Impedance of Moderately Fat Transmitting Crossed-Monopole Antennas, M.S. E.E. Thesis, Naval Postgraduate School, Monterey, California, March 1976.

INITIAL DISTRIBUTION LIST

1.	Defense Documentation Center Cameron Station Alexandria, Virginia 22314	2
2.	Library, Code 0212 Naval Postgraduate School Monterey, California 93940	2
3.	Department Chairman, Code 62 Department of Electrical Engineering Naval Postgraduate School Monterey, California 93940	1
4.	Assoc. Prof. R W. Burton, Code 62Zn Department of Electrical Engineering Naval Postgraduate School Monterey, California 93940	15
5.	LT William E. Beyatte Field Command, Defense Nuclear Agency Livermore Branch PO Box 808(L-395) Livermore, California 94550	1
6.	Post-Doctoral Program RADC-RBC Rome Air Development Center Griffiss AFB New York 13441	1

7. Mr. Phillip Blacksmith 1
Code LZR
Air Force Research Lab.
Laurence G. Hanscom Field
Bedford, Massachusetts 01730

8. Air Force Weapons Laboratory/PRP 2
Kirtland AFB
New Mexico 87117

Thesis
B505 Beyatte
c.1 Charge and current density distributions on moderately thick transmitting crossed-monopole antennas.
167931